

# DATA-DRIVEN CONSTRUCTION OF FINITE ABSTRACTIONS FOR INTERCONNECTED SYSTEMS: A COMPOSITIONAL APPROACH

DANIEL AJELEYE AND MAJID ZAMANI

ABSTRACT. Finite-state abstractions (a.k.a. *symbolic models*) present a promising avenue for the formal verification and synthesis of controllers in continuous-space control systems. These abstractions provide simplified models that capture the fundamental behaviors of the original systems. However, the creation of such abstractions typically relies on the availability of precise knowledge concerning system dynamics, which might not be available in many real-world applications. In this work, we introduce an innovative, data-driven, and compositional approach to generate finite abstractions for interconnected systems that consist of discrete-time control subsystems with unknown dynamics. These subsystems interact through an unknown static interconnection map. Our methodology for abstracting the interconnected system involves constructing abstractions for individual subsystems and incorporating an abstraction of the interconnection map. Within our data-driven framework, we collect data samples from unknown subsystems and collect input-output data from the interconnection map to construct finite abstractions while ensuring their correctness. Nevertheless, the computational complexity of building finite abstractions for interconnected systems based on those of subsystems can still become formidable, especially depending on the structure of the interconnection map. To address this challenge, we introduce intermediate variables that streamline the process, breaking down the interconnection and abstraction tasks into more manageable computations. To demonstrate the effectiveness of our approach, we present results for two numerical benchmarks: the construction of a finite abstraction for a 32-dimensional system by combining abstractions of 32 scalar subsystems, and the synthesis of a controller for an 8-dimensional system based on its constructed finite abstraction, aimed at achieving a consensus objective.

## 1. INTRODUCTION

Designing controllers for continuous-space systems with complex control objectives presents a formidable challenge. Fortunately, recent advances have introduced several techniques to address these obstacles. A particularly effective approach involves the creation of finite abstractions for the original control systems [Tab09]. These abstractions provide concise representations of dynamical systems, designed in such a way that a discrete controller, initially constructed to enforce specific properties on the finite model, can be further refined into a hybrid controller that upholds these properties on the actual concrete system. However, the process of constructing symbolic models for large-scale systems composed of many subsystems is inherently intricate. To overcome this challenge, an effective strategy is to begin by constructing symbolic models for individual subsystems. Subsequently, through a compositional framework, one can assemble a finite abstraction of the entire network by integrating these individual abstractions.

In this work, we introduce a novel data-driven technique for constructing a finite abstraction of a system composed of smaller interacting components, *i.e.*, subsystems. In particular, our approach entails the collection of data from multiple initializations of these unknown subsystems, thereby enabling us to construct a data-driven finite abstraction for each individual subsystem. This abstraction process is performed concurrently and independently, as each subsystem's internal state remains isolated from the others through input-state interfaces. The interplay between these subsystems is governed by an interconnection map, which constraints the values of internal variables spanning the various subsystems.

---

This work was supported by the NSF under grant CNS-2145184.

Furthermore, the interconnection maps are also approximated by finite abstractions. We present a compositional result, which demonstrates the existence of a feedback refinement relation [RWR16] that bridges the abstract interconnections with the concrete ones. Borrowing insights from [GKA17], we introduce a sparsity constraint to the data-driven approximation of the interconnection map, resulting in a sparse matrix representation of the nonlinear interconnection map. This approach facilitates the incorporation of latent variables, capturing intermediate computations, and thus breaking down the interconnection and abstraction tasks into more manageable components. Ultimately, this approach significantly reduces the overall complexity of the abstraction process. Finally, we illustrate the efficacy of our approach by applying it to two numerical benchmarks: the construction of a finite abstraction for a 32-dimensional system by combining abstractions of 32 scalar subsystems, and the synthesis of a controller for an 8-dimensional system based on its constructed finite abstraction, aimed at achieving a consensus objective.

**Related Work.** Limited research has been dedicated to constructing finite abstractions using data-driven methods. These findings encompass various systems, including unknown monotone systems [MGF21], incrementally input-to-state stable control systems [LF22], and continuous-time perturbed systems [KMS<sup>+</sup>22]. Furthermore, approaches like [XZEL20, FQMV17, CPMJ22] focus predominantly on data-driven techniques for verifying unknown systems while offering probabilistic guarantees. However, it is crucial to recognize that all of these aforementioned results adopt a monolithic perspective, abstracting the entire system. It is important to acknowledge that the monolithic abstraction approach encounters scalability issues. These issues stem from the exponential increase in complexity based on the number of state variables in the model, primarily because of the gridding of state sets. As a consequence, these techniques tend to face computational limitations, especially in state spaces that exceed four dimensions.

Our approach is applicable to all classes of non-linear discrete-time control systems, in contrast to the work by [MGF21], which is exclusively suited for monotone systems. While the result in [LF22] imposes incremental stability requirements on the underlying systems, and similar to [XZEL20], [FQMV17] and [CPMJ22] provide finite abstractions with probabilistic guarantees, our approach stands out by offering a compositional construction of sound abstractions with a 100% correctness guarantee. Importantly, our method does not necessitate any stability assumptions on the subsystems, nor does it impose any implicit conditions regarding the number of subsystems.

In recent years, significant progress has been made in developing a compositional framework for the construction of finite abstractions for networks of control systems. Noteworthy contributions in the literature include [HAT17, KAZ18, MGW17], which construct sound symbolic models of interconnected systems in a compositional manner. Regrettably, all of these works on the compositional construction of finite abstractions require the availability of system models, which are often absent in many real-world applications. To address this challenge, one might explore various *indirect data-driven* strategies to come up with models for unknown dynamical systems through identification techniques (*e.g.*, [Lju98, FS18, HW13] and references therein). However, obtaining an accurate model can be arduous, time-intensive, and computationally expensive in itself.

## 2. PRELIMINARIES AND DEFINITIONS

**2.1. Notation.** Symbols  $\mathbb{R}$ ,  $\mathbb{R}_{>0}$ , and  $\mathbb{R}_{\geq 0}$ , respectively, represent sets of real, positive, and non-negative real numbers. Notations  $\cup$ ,  $\cap$ , and  $\setminus$  indicate, respectively, set union, intersection, and set difference. Similarly,  $\wedge$  denotes the logical conjunction. The symbol  $\mathbb{N}$  denotes the set of natural numbers and  $\forall n \in \mathbb{N} \cup \{0\}$ , symbol  $\mathbb{N}_{\geq n} = \{l \in \mathbb{N} \cup \{0\} \mid l \geq n\}$ . In the case where  $a, b \in \mathbb{N}_{\geq 0}$  and  $a < b$ , we employ the notations  $[a; b]$ ,  $(a; b)$ ,  $[a; b)$ , and  $(a; b]$  to represent respectively the closed, open, half-open from the right, and half-open from the left intervals in  $\mathbb{N}_{\geq 0}$ . Alternatively, for  $a, b \in \mathbb{R}$  and  $a < b$ , we use  $[a, b]$ ,  $(a, b)$ ,  $[a, b)$ , and  $(a, b]$  to denote the corresponding intervals in  $\mathbb{R}$ . For any non-empty set  $Q$  and  $n \in \mathbb{N}$ , we denote the cardinality of  $Q$  as  $\mathcal{C}_a(Q)$ , while  $Q^n$  indicates the Cartesian product of  $n$  duplicates of  $Q$ . Given  $N$  vectors  $x_i \in \mathbb{R}^{n_i}$ ,  $n_i \in \mathbb{N}$ , and  $i \in \{1, \dots, N\}$ , we use  $x = [x_1; \dots; x_N]$  to denote the corresponding column vector of dimension  $\sum_i n_i$ . The vector  $\mathbf{1}_n \in \mathbb{R}^n$  is defined as  $[1; 1; \dots; 1] \in \mathbb{R}^n$ . Notation  $\dim(Z) \in \mathbb{N}_{\geq 0}$  denotes the dimension of a given set  $Z$

within a vector space. For any  $\bar{p}, \bar{q} \in \mathbb{R}^n$  and relational operator  $\simeq \in \{\leq, <, =, >, \geq\}$ , where  $\bar{p} = [p_1; \dots; p_n]$  and  $\bar{q} = [q_1; \dots; q_n]$ ,  $\bar{p} \simeq \bar{q}$  is interpreted as  $p_l \simeq q_l, \forall l \in \{1, \dots, n\}$ , *i.e.*, component-wise comparison. Assuming  $\bar{p} < \bar{q}$ , then the *compact hyper-interval*  $[\bar{p}, \bar{q}]$  is given as  $[p_1, q_1] \times \dots \times [p_n, q_n]$ . Furthermore, given  $c = [c_1; \dots; c_n] \in \mathbb{R}^n$ , we define the sum  $\oplus$  as  $c \oplus [\bar{p}, \bar{q}] := [p_1 + c_1, c_1 + q_1] \times \dots \times [p_n + c_n, c_n + q_n]$ . Notation  $|c|$  means the entry-wise absolute value of  $c \in \mathbb{R}^n$  *i.e.*,  $[|c_1|; \dots; |c_n|]$ , while  $\|c\|$  means the infinity norm of  $c$ . Similarly,  $\|c\|_p$  gives the  $\ell_p$ -norm of  $c$  for some  $p \geq 1$ . For any  $\bar{r} \in \mathbb{R}_{>0}^n$  and  $c_0 \in \mathbb{R}^n$ , notation  $\Phi_{\bar{r}}(c_0)$  is interpreted as  $c_0 \oplus [-\bar{r}, \bar{r}]$ . For a given compact hyper-interval  $H$  and discretization parameter vector  $\eta_h \in \mathbb{R}_{>0}^n$ , we create a partition of  $H$  into cells  $\Phi_{\eta_h}(h)$  such that  $H \subseteq \bigcup_{h \in [H]_{\eta_h}} \Phi_{\eta_h}(h)$ , where  $[H]_{\eta_h}$  represents a finite set of representative points selected from those partition sets. For any  $\vartheta \in \mathbb{R}^{n \times m}$ ,  $\|\vartheta\|$  denotes the infinity norm of  $\vartheta$ .

**2.2. Discrete-Time Control Systems.** Here, we investigate discrete-time control systems (cf. next definition) encompassing both internal and external inputs. Internal variables facilitate interconnection with other systems, whereas external ones serve as interfaces for controllers.

**Definition 2.1.** A discrete-time control system (dt-CS)  $\Xi$  is represented via a tuple

$$(2.1) \quad \Xi = (\mathcal{X}, U, \mathcal{U}, f),$$

where  $\mathcal{X}, U$ , and  $\mathcal{U}$  denote the state set, external input set, and internal input set of the control system, respectively. These sets are assumed to be nonempty subsets of normed vector spaces with finite dimensions. The transition function, denoted as  $f : \mathcal{X} \times U \times \mathcal{U} \rightrightarrows \mathcal{X}$ , is a set-valued map. The dt-CS  $\Xi$  is characterized by difference inclusions of the following form:

$$(2.2) \quad x(k+1) \in f(x(k), u(k), w(k)),$$

where at time  $k \in \mathbb{N}$ ,  $x(k) \in \mathcal{X}$ ,  $u(k) \in U$ , and  $w(k) \in \mathcal{U}$  represent the state, external, and internal input, respectively.

A dt-CS  $\Xi = (\mathcal{X}, U, \mathcal{U}, f)$  is referred to as *deterministic* when  $\mathcal{C}_d(f(x, u, w))$  is at most 1  $\forall x \in \mathcal{X}, \forall u \in U$ , and  $\forall w \in \mathcal{U}$ . Otherwise, the dt-CS  $\Xi$  is considered *non-deterministic*. In addition,  $\Xi$  is classified as *finite* if  $\mathcal{X}, U$ , and  $\mathcal{U}$  are finite sets, and  $\Xi$  is said to be *infinite* otherwise.

*Remark 2.2.* If a dt-CS  $\Xi$  does not have internal inputs, the tuple (2.1) in Definition 2.1 simplifies to a *simple system*

$$(2.3) \quad \Xi = (X, U, f),$$

where the set-valued map  $f$  becomes  $f : X \times U \rightrightarrows X$ . Consequently, the formulation in (2.2) is reduced to:

$$(2.4) \quad x(k+1) \in f(x(k), u(k)).$$

Subsequently, we utilize the notion of the dt-CS in equations (2.3) and (2.4), to specifically refer to an interconnected dt-CS. This dt-CS is constructed by interconnecting several subsystems described as in (2.1) and (2.2). Next, we introduce the notion of feedback refinement relation, which provides a relation between two dt-CSs in terms of controller synthesis.

**2.3. Feedback Refinement Relations.** Here, we recall the notion of feedback refinement relations [RWR16] that establish a relationship between two dt-CSs, as described in Definition 2.1 and quantify the relationship between them in terms of controller synthesis [Tab09].

**Definition 2.3.** Consider two dt-CS  $\Xi_i = (\mathcal{X}_i, U_i, \mathcal{U}_i, f_i)$ , where  $i \in \{1, 2\}$ , such that  $U_2 \subseteq U_1$ . There is a feedback refinement relation from  $\Xi_1$  to  $\Xi_2$  if there exist nonempty relations  $\mathcal{Q} \subseteq \mathcal{X}_1 \times \mathcal{X}_2$  and  $\mathcal{R} \subseteq \mathcal{U}_1 \times \mathcal{U}_2$  such that,  $\forall (x_1, x_2) \in \mathcal{Q} \forall w_1 \in \mathcal{U}_1 \exists w_2 \in \mathcal{U}_2$  such that  $(w_1, w_2) \in \mathcal{R}$  and the next two conditions hold:

- $U_{\Xi_2}(x_2, w_2) \subseteq U_{\Xi_1}(x_1, w_1)$ , where  $U_{\Xi_i}(x_i, w_i) := \{u_i \in U_i \mid f_i(x_i, u_i, w_i) \neq \emptyset\}$  is the set of *admissible* external inputs for state  $x_i \in \mathcal{X}_i$  and internal input  $w_i \in \mathcal{U}_i, \forall i \in \{1, 2\}$ ;

- if  $u \in U_{\Xi_2}(x_2, w_2)$ , then  $Q(f_1(x_1, u, w_1)) \subseteq f_2(x_2, u, w_2)$ .

Furthermore, whenever there is a feedback refinement relation as in Definition 2.3 from dt-CS  $\Xi_1$  to  $\Xi_2$ , we denote it by  $\Xi_1 \preceq_Q \Xi_2$ . When there are no internal inputs, Definition 2.3 simplifies to the next one.

**Definition 2.4.** Consider two dt-CSs  $\Xi_i = (X_i, U_i, f_i)$ , where  $i \in \{1, 2\}$ , such that  $U_2 \subseteq U_1$ . There is a feedback refinement relation from  $\Xi_1$  to  $\Xi_2$  if there exists a nonempty relation  $Q \subseteq X_1 \times X_2$  such that,  $\forall (x_1, x_2) \in Q$  the following two conditions hold:

- $U_{\Xi_2}(x_2) \subseteq U_{\Xi_1}(x_1)$ , where  $U_{\Xi_i}(x_i) := \{u_i \in U_i \mid f_i(x_i, u_i) \neq \emptyset\}$  is the *admissible* input set for state  $x_i \in X_i$ ,  $\forall i \in \{1, 2\}$ ;
- if  $u \in U_{\Xi_2}(x_2)$ , then  $Q(f_1(x_1, u)) \subseteq f_2(x_2, u)$ .

### 3. SYSTEMS INTERCONNECTION

In this section, our focus lies in the analysis of interconnected systems, comprised of several dt-CSs.

**3.1. Interconnected dt-CSs.** Now, we define an interconnection of several dt-CSs.

**Definition 3.1.** Consider  $N \in \mathbb{N}_{\geq 1}$  dt-CSs  $\Xi_i = (\mathcal{X}_i, U_i, \mathcal{U}_i, f_i)$ , where  $i \in [1; N]$ . An interconnection  $\mathcal{I}$  between the  $N$  subsystems is defined by the tuple  $\mathcal{I} = (\prod_{i=1}^N \mathcal{X}_i, \prod_{i=1}^N \mathcal{U}_i, \mathcal{M})$ , where  $\mathcal{M}$  is the interconnection map and defined as,

$$(3.1) \quad \mathcal{M} : \prod_{i=1}^N \mathcal{X}_i \rightarrow \prod_{i=1}^N \mathcal{U}_i.$$

For the sake of simple presentation, an interconnection  $\mathcal{I}$  as in Definition 3.1 is concisely written as tuple  $\mathcal{I} = (\mathcal{X}^{\mathcal{I}}, \mathcal{U}^{\mathcal{I}}, \mathcal{M})$  where  $\mathcal{X}^{\mathcal{I}} = \prod_{i=1}^N \mathcal{X}_i$  and  $\mathcal{U}^{\mathcal{I}} = \prod_{i=1}^N \mathcal{U}_i$ . Next, we define the interconnected dt-CS.

**Definition 3.2.** Consider a collection of  $N \in \mathbb{N}_{\geq 1}$  subsystems  $\Xi_i = (\mathcal{X}_i, U_i, \mathcal{U}_i, f_i)$ , where  $i \in [1; N]$ , along with an interconnection  $\mathcal{I} = (\mathcal{X}^{\mathcal{I}}, \mathcal{U}^{\mathcal{I}}, \mathcal{M})$  that defines the coupling among these subsystems. The interconnected dt-CS  $\Xi = (X, U, f)$  is denoted by  $\mathcal{I}(\Xi_1, \dots, \Xi_N)$ , and defined as follows:

- $X = \prod_{i=1}^N \mathcal{X}_i$  and  $U = \prod_{i=1}^N U_i$ ;
- for any state  $x = [x_1; \dots; x_N] \in X$  and input  $u = [u_1; \dots; u_N] \in U$ , it holds that

$$(3.2) \quad f(x, u) := \{[x'_1; \dots; x'_N] \mid x'_i \in f_i(x_i, u_i, w_i) \forall i \in [1; N]\},$$

where  $[w_1; \dots; w_N] = \mathcal{M}([x_1; \dots; x_N])$ .

Definitions 3.1 and 3.2 highlight the role of internal inputs within a network of dt-CSs. These internal variables facilitate the construction of independent abstractions for subsystems.

The following definition introduces a notion of abstract interconnection.

**Definition 3.3.** Consider interconnections  $\mathcal{I}_i = (\mathcal{X}^{\mathcal{I}_i}, \mathcal{U}^{\mathcal{I}_i}, \mathcal{M}_i)$ , where  $i \in \{1, 2\}$  such that  $\dim(\mathcal{X}^{\mathcal{I}_1}) = \dim(\mathcal{X}^{\mathcal{I}_2})$  and  $\dim(\mathcal{U}^{\mathcal{I}_1}) = \dim(\mathcal{U}^{\mathcal{I}_2})$ . Interconnection  $\mathcal{I}_2$  is called an abstraction of  $\mathcal{I}_1$  if there exist relations  $\tilde{Q} \subseteq \mathcal{X}^{\mathcal{I}_1} \times \mathcal{X}^{\mathcal{I}_2}$  and  $\tilde{\mathcal{R}} \subseteq \mathcal{U}^{\mathcal{I}_1} \times \mathcal{U}^{\mathcal{I}_2}$  such that  $\forall (x, \hat{x}) \in \tilde{Q} \forall w \in \mathcal{M}(x) \exists \hat{w} \in \tilde{\mathcal{M}}(\hat{x})$  such that  $(w, \hat{w}) \in \tilde{\mathcal{R}}$ .

The mentioned interconnection abstraction is employed to construct abstractions of interconnected dt-CSs using the subsystems' abstractions compositionally. Next subsection introduces the main problem which we aim at solving.

**3.2. Problem Formulation.** In this work, we assume that we have  $N$  infinite, deterministic dt-CSs denoted by  $\Xi_i$ , as described in (2.1) and (2.2), where  $i \in [1; N]$ . The transition maps  $f_i$  in (2.2) are considered to be *unknown*. Furthermore, these  $N$  subsystems are interconnected via an interconnection map  $\mathcal{M}$  as in Definition 3.1 which is assumed to be *unknown* as well.

The primary objective of this work is to construct a finite abstraction of an interconnection of  $N$  dt-CSs  $\Xi_i$ , for the sake of synthesizing controllers using the constructed abstraction. In our setting, although the underlying dynamics of  $\Xi_i$  (denoted by  $f_i$  in (2.2)) are unknown, we assume that sampled data points from their trajectories are available. We gather these data samples in a set  $\mathcal{D}_{\mathcal{N}_{C_i}} := \{(x_l, u_l, w_l, x'_l) \mid x'_l = f_i(x_l, u_l, w_l)\}$  where  $x_l \in \mathcal{X}_i$ ,  $u_l \in \mathcal{U}_i$ , and  $w_l \in \mathcal{W}_i$ ,  $l \in [1; \mathcal{N}_{C_i}]$ . Note that we abuse notation by using  $x_l$  and  $w_l$  later to represent the data point for the state of the interconnected dt-CSs and the vector containing all internal inputs, respectively (cf. Subsection 4.2). Although the interconnection map in (3.1) is presumed to be an unknown nonlinear function, we possess a sufficient set of input-output data points for this mapping. These collected data-points are stored in the set  $\mathcal{D}_{\mathcal{N}_I} := \{(x_l, w_l) \in \mathcal{X}^I \times \mathcal{W}^I \mid w_l = \mathcal{M}(x_l), l \in [1; \mathcal{N}_I]\}$ . Under these assumptions, we formulate the main problem that we aim to address in this work.

**Problem 3.4.** Consider an interconnected dt-CS  $\Xi$  as in Definition 3.2 composed of  $N$  subsystems  $\Xi_i$ ,  $i \in [1; N]$ , where transition maps  $f_i$  and the interconnection map  $\mathcal{M}$  are unknown. Develop a compositional, data-driven approach based on the sets of data  $\mathcal{D}_{\mathcal{N}_{C_i}}$ ,  $i \in [1; N]$ , and  $\mathcal{D}_{\mathcal{N}_I}$ , to construct a finite abstraction  $\hat{\Xi}$  such that  $\Xi \preceq_Q \hat{\Xi}$ , where  $Q$  is a feedback refinement relation.

In the next section, we introduce a data-driven approach for constructing abstractions of subsystems within a network and the interconnection abstraction as in Definition 3.3.

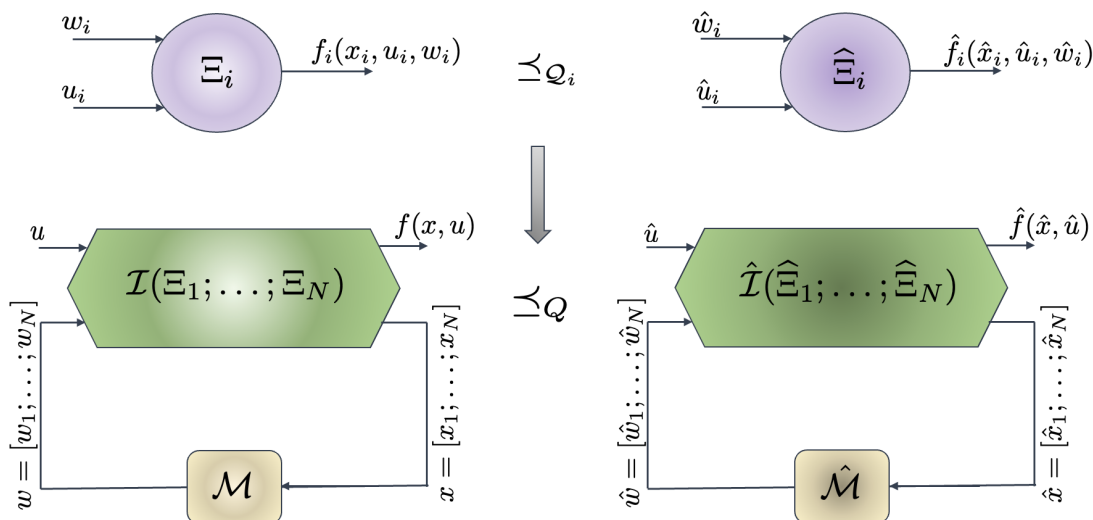


FIGURE 1. Interconnection of  $N$  finite abstractions  $\hat{\Xi}_i$  while maintaining the feedback refinement relation  $Q$ . This interconnection is achieved by leveraging the compositionality result (cf. Theorem 4.10).

#### 4. DATA-DRIVEN CONSTRUCTION OF FINITE ABSTRACTIONS

In this section, we tackle Problem 3.4 in a step-by-step fashion, commencing with the creation of finite abstractions for individual subsystems. Then, we develop a finite approximation of the interconnection.

Finally, we integrate these constructed subsystem abstractions and the interconnection approximation to construct an overall abstraction, encompassing the behavior of the entire interconnected system.

**4.1. Symbolic Abstractions for Subsystems.** Consider  $N$  dt-CSs  $\Xi_i = (\mathcal{X}_i, U_i, \mathcal{U}_i, f_i)$ , where  $i \in [1; N]$ , which are interconnected by a map  $\mathcal{M}$ . To tackle Problem 3.4, we first raise the following assumptions.

**Assumption 1.** For any  $u \in U_i$ , the transition map  $f_i$  is Lipschitz continuous with respect to  $x$  and  $w$ , with Lipschitz constants  $\mathcal{L}_{x_i}(u)$  and  $\mathcal{L}_{w_i}(u)$ , respectively, for all  $i \in [1; N]$ .

**Assumption 2.** The interconnection map  $\mathcal{M}$  is Lipschitz continuous with a Lipschitz constant  $\mathcal{L}_{\mathcal{M}}$ .

*Remark 4.1.* Note that the results presented in [WZ96] can be employed to estimate the Lipschitz constants mentioned in Assumption 1 and 2 for the unknown maps. This estimation is achieved by utilizing finite data sets  $\mathcal{D}_{\mathcal{N}_{C_i}}$  and  $\mathcal{D}_{\mathcal{N}_{I_i}}$ , obtained from the unknown interconnected system. Nevertheless, in this work, we assume that we know precise estimates of the Lipschitz constants. As a result, we do not consider any confidence over the estimations of these constants. For implementation details, Appendix-A provides an elaboration on the estimation process for the Lipschitz constants mentioned in Assumptions 1 and 2. This process involves leveraging finite datasets,  $\mathcal{D}_{\mathcal{N}_C}$  and  $\mathcal{D}_{\mathcal{N}_I}$ , collected from the unknown system.

For simplicity, in the remainder of this subsection we omit the index  $i$  from the representations of the subsystems. Let us denote by  $\eta_x \in (\mathbb{R}_{>0})^{\dim(\mathcal{X})}$ ,  $\eta_u \in (\mathbb{R}_{>0})^{\dim(U)}$  and  $\eta_w \in (\mathbb{R}_{>0})^{\dim(\mathcal{U})}$  the discretization parameters for  $\mathcal{X}$ ,  $U$ , and  $\mathcal{U}$ , respectively. Hence, we generate symbolic state set  $\hat{\mathcal{X}} := [\mathcal{X}]_{\eta_x}$ ,  $\hat{U} := [U]_{\eta_u}$ , and  $\hat{\mathcal{U}} := [\mathcal{U}]_{\eta_w}$ . Accordingly, the exact reachable set of states from a grid cell centered at  $\hat{x} \in \hat{\mathcal{X}}$ , under an internal input grid cell centered at  $\hat{w} \in \hat{\mathcal{U}}$ , and under an external input  $\hat{u} \in \hat{U}$ , is defined as  $\mathbf{R}(\hat{x}, \hat{u}, \hat{w}) := \{f(x, \hat{u}, w) \mid x \in \Phi_{\eta_x/2}(\hat{x}) \text{ and } w \in \Phi_{\eta_w/2}(\hat{w})\}$ . Our objective is to construct an over-approximation of  $\mathbf{R}(\hat{x}, \hat{u}, \hat{w})$  for any  $(\hat{x}, \hat{u}, \hat{w}) \in \hat{\mathcal{X}} \times \hat{U} \times \hat{\mathcal{U}}$  using a function called *growth bound*, formally defined as follows.

**Definition 4.2.** Given a dt-CS  $\Xi = (\mathcal{X}, U, \mathcal{U}, f)$  with corresponding symbolic sets  $\hat{\mathcal{X}}$ ,  $\hat{U}$ , and  $\hat{\mathcal{U}}$ , a function  $\kappa : \mathbb{R}_{\geq 0}^{\dim(\mathcal{X})} \times \hat{\mathcal{X}} \times \hat{U} \times \hat{\mathcal{U}} \rightarrow \mathbb{R}_{\geq 0}^{\dim(\mathcal{X})}$  satisfying

$$(4.1) \quad |x'_1 - x'_2| \leq \kappa(|x_1 - x_2|, \hat{x}, \hat{u}, \hat{w}),$$

where  $x'_1 = f(x_1, \hat{u}, w_1)$  and  $x'_2 = f(x_2, \hat{u}, w_2)$ , for any  $x_1, x_2 \in \Phi_{\eta_x/2}(\hat{x})$ ,  $w_1, w_2 \in \Phi_{\eta_w/2}(\hat{w})$ , is called a *growth bound* of  $\Xi$ .

We now formally define finite abstractions of subsystems.

**Definition 4.3.** Given a dt-CS  $\Xi = (\mathcal{X}, U, \mathcal{U}, f)$  and a growth bound  $\kappa$ , a finite dt-CS  $\hat{\Xi} = (\hat{\mathcal{X}}, \hat{U}, \hat{\mathcal{U}}, \hat{f})$  is a finite abstraction of  $\Xi$ , with the transition map  $\hat{f} : \hat{\mathcal{X}} \times \hat{U} \times \hat{\mathcal{U}} \rightrightarrows \hat{\mathcal{X}}$  if for any  $\hat{x} \in \hat{\mathcal{X}}$ ,  $\hat{w} \in \hat{\mathcal{U}}$  and  $\hat{u} \in \hat{U}$ ,  $\hat{x}' \in \hat{f}(\hat{x}, \hat{u}, \hat{w})$  for all  $\hat{x}' \in \hat{\mathcal{X}}$  where  $(f(\hat{x}, \hat{u}, \hat{w}) \oplus [-q', q']) \cap \Phi_{\eta_x/2}(\hat{x}') \neq \emptyset$ , with  $q' = \kappa(\eta_x, \hat{x}, \hat{u}, \hat{w})$ .

In addition, we present the following theorem, which shows the usefulness of finite abstractions in Definition 4.3 by establishing a feedback refinement relation (namely set membership relation) between a concrete dt-CS and its finite abstraction. Establishing a feedback refinement relation [RWR16] between a dt-CS and its finite abstraction ensures that any robust controller designed for the abstraction, which enforces a specification (*e.g.*, LTL [BK08],  $\omega$ -regular properties described by universal co-Büchi automata [AZ24], reach-avoid [AMP22], *e.t.c.*) can be refined back to the dt-CS to achieve the same specification.

**Theorem 4.4.** Consider a dt-CS as in Definition 2.1, and let  $\hat{\Xi} = (\hat{\mathcal{X}}, \hat{U}, \hat{\mathcal{U}}, \hat{f})$  be its finite abstraction according to Definition 4.3. Then  $\Xi \preceq_{\mathcal{Q}} \hat{\Xi}$ , where the feedback refinement relation  $\mathcal{Q}$  is defined as  $(x, \hat{x}) \in \mathcal{Q}$  if  $x \in \Phi_{\eta_x/2}(\hat{x})$ .

The proof is similar to that of [RWR16, Theorem VIII.4] and is omitted here. Remark that a version of the growth bound satisfying (4.1) is introduced in [RWR16] for model-based and continuous-time settings.

However, considering scenarios where the subsystem dynamics is unknown and to reduce the dependency on the subsystem dynamics, we adopt a parametrized function [KMS<sup>+</sup>22, ALZ23] presented in (4.2), as a candidate growth bound.

For any  $\bar{r} \in \mathbb{R}_{\geq 0}^{\dim(\mathcal{X})}$ ,  $\hat{x} \in \hat{\mathcal{X}}$ ,  $\hat{u} \in \hat{U}$  and  $\hat{w} \in \hat{\mathcal{U}}$ , we present the parametrized candidate growth bound as follows:

$$(4.2) \quad \kappa_{\vartheta}(\bar{r}, \hat{x}, \hat{u}, \hat{w}) := \vartheta_1(\hat{x}, \hat{u}, \hat{w})\bar{r} + \vartheta_2(\hat{x}, \hat{u}, \hat{w}),$$

where  $\vartheta_1 \in \mathbb{R}_{\geq 0}^{\dim(\mathcal{X}) \times \dim(\mathcal{X})}$ ,  $\vartheta_2 \in \mathbb{R}_{\geq 0}^{\dim(\mathcal{X})}$ , and  $\vartheta \in \mathbb{R}_{\geq 0}^p$  is a column vector formed by stacking those of  $\vartheta_1$  and  $\vartheta_2$ , with  $p = \dim(\mathcal{X})(\dim(\mathcal{X}) + 1)$ . Remark that for every abstract state, parameters of  $\vartheta_1$  and  $\vartheta_2$  are locally defined, resulting in a less conservative growth bound. The following lemma, the proof of which is provided in Appendix B, plays a pivotal role in demonstrating the results of Theorem 4.6 later on.

**Lemma 4.5.** *Consider a pair  $(\hat{u}, \hat{w}) \in \hat{U} \times \hat{\mathcal{U}}$ . By Assumption 1, suppose that for any  $x_1, x_2 \in \Phi_{\eta_x/2}(\hat{x})$ ,  $w_1, w_2 \in \Phi_{\eta_w/2}(\hat{w})$ ,*

$$(4.3) \quad \|f(x_1, \hat{u}, w_1) - f(x_2, \hat{u}, w_2)\| \leq \mathcal{L}_x(\hat{u})\|x_1 - x_2\| + \mathcal{L}_w(\hat{u})\|w_1 - w_2\|.$$

Then one obtains

$$(4.4) \quad \|\vartheta_1(\hat{x}, \hat{u}, \hat{w})\| \leq \mathcal{L}_x(\hat{u}), \quad \forall \hat{x} \in \hat{\mathcal{X}}, \forall \hat{u} \in \hat{U} \text{ and } \forall \hat{w} \in \hat{\mathcal{U}}.$$

We now present a data-driven approach utilizing data set  $\mathcal{D}_{\mathcal{N}_C}$  to compute a candidate growth bound as in (4.2). Our approach also offers a formal correctness guarantee for (4.2) implying that it is a growth bound for dt-CS in (2.2) (cf. Theorem 4.6). The primary objective is to seek a growth bound that is less conservative in terms of over-approximating the reachable sets. In our proposed framework, we initially formulate the candidate growth bound in (4.2) as the following robust convex program:

$$(4.5) \quad \text{RCP: } \begin{cases} \min_{\vartheta} & \mathbf{1}_p^\top \vartheta \\ \text{s.t.} & \vartheta \in [0, \bar{\vartheta}], \forall x_1, x_2 \in \Phi_{\eta_x/2}(\hat{x}), \\ & \forall w_1, w_2 \in \Phi_{\eta_w/2}(\hat{w}), \\ & |x'_1 - x'_2| - \kappa_{\vartheta}(|x_1 - x_2|, \hat{x}, \hat{u}, \hat{w}) \leq 0, \end{cases}$$

where  $x'_1 = f(x_1, \hat{u}, w_1)$ ,  $x'_2 = f(x_2, \hat{u}, w_2)$ ,  $p = \dim(\mathcal{X})(\dim(\mathcal{X}) + 1)$ , and  $\bar{\vartheta} \in \mathbb{R}_{> 0}^p$  is a sufficiently large vector component-wise.

One can readily verify that a feasible solution of the RCP in (4.5) provides a growth bound as in (4.1) for dt-CS in (2.2). Unfortunately, a precise knowledge of the dynamic is required for solving the problem. To resolve these issues, we collect data samples from trajectories of unknown dt-CS and propose a scenario convex program (SCP) corresponding to the original RCP. To do so, consider a set of  $\mathcal{N}_C$  data points  $\mathcal{D}_{\mathcal{N}_C}$  collected within cells  $\Phi_{\hat{\eta}_x/2}(\tilde{x})$  where  $\tilde{x} \in [\Phi_{\eta_x/2}(\hat{x})]_{\hat{\eta}_x}$ , which are sub-grids themselves within the cell  $\Phi_{\eta_x/2}(\hat{x})$ , where  $\hat{\eta}_x := \frac{1}{\dim(\mathcal{X})\sqrt{\mathcal{N}_C}}\eta_x$  (cf. Fig. (2)). The proposed size of the sub-grid cells is due to extracting  $\mathcal{N}_C$  data points from the primary cell  $\Phi_{\eta_x/2}(\hat{x})$ , which has a dimension of  $\dim(\mathcal{X})$ . By leveraging the data set  $\mathcal{D}_{\mathcal{N}_C}$ , for any  $(\hat{x}, \hat{u}, \hat{w}) \in \hat{\mathcal{X}} \times \hat{U} \times \hat{\mathcal{U}}$ , we propose the SCP associated to the RCP in (4.5) for a cell  $\Phi_{\eta_x/2}(\hat{x})$  as

$$(4.6) \quad \text{SCP: } \begin{cases} \min_{\vartheta} & \mathbf{1}_p^\top \vartheta \\ \text{s.t.} & \vartheta \in [0, \bar{\vartheta}], \forall l, \bar{l} \in \{1, \dots, \mathcal{N}_C\}, \\ & |x'_l - x'_{\bar{l}}| - \vartheta_1(\hat{x}, \hat{u}, \hat{w})|x_l - x_{\bar{l}}| - \vartheta_2(\hat{x}, \hat{u}, \hat{w}) + \varrho \leq 0, \end{cases}$$

where  $\varrho \in \mathbb{R}_{\geq 0}^{\dim(\mathcal{X})}$  can be obtained as outlined in the following theorem.

**Theorem 4.6.** Consider a dt-CS  $\Xi = (\mathcal{X}, U, \mathcal{U}, f)$ . For any  $(\hat{x}, \hat{u}, \hat{w}) \in [\mathcal{X}]_{\eta_x} \times [U]_{\eta_u} \times [\mathcal{U}]_{\eta_w}$ , suppose for a cell  $[\Phi_{\eta_x/2}(\hat{x})]$ ,  $[\Phi_{\eta_x/2}(\hat{x})]_{\hat{\eta}_x}$  is constructed where  $\hat{\eta}_x := \frac{1}{\dim(\mathcal{X})\sqrt{\mathcal{N}_C}}\eta_x$ . Then, the solution of (4.6) provides a growth bound as in (4.1) corresponding to  $(\hat{x}, \hat{u}, \hat{w})$ , where

$$(4.7) \quad \varrho := 2\mathcal{L}_x(\hat{u})\hat{\eta}_x + \mathcal{L}_w(\hat{u})\|\eta_w\|\mathbf{1}_{\dim(\mathcal{X})},$$

$\mathcal{L}_x(\hat{u})$  and  $\mathcal{L}_w(\hat{u})$  are Lipschitz constants as in Assumption 1.

*Proof.* It can be readily verified that the optimization problem (4.6) admits a feasible solution. For any fixed  $(\hat{x}, \hat{u}, \hat{w}) \in [\mathcal{X}]_{\eta_x} \times [U]_{\eta_u} \times [\mathcal{U}]_{\eta_w}$ , let

$$\begin{aligned} \beta(\vartheta, x_1, x_2, w_1, w_2) &:= |f(x_1, \hat{u}, w_1) - f(x_2, \hat{u}, w_2)| \\ &\quad - \vartheta_1(\hat{x}, \hat{u}, \hat{w})|x_1 - x_2| - \vartheta_2(\hat{x}, \hat{u}, \hat{w}), \end{aligned}$$

for any  $x_1, x_2 \in \Phi_{\eta_x/2}(\hat{x})$  and  $w_1, w_2 \in \Phi_{\eta_w/2}(\hat{w})$ . In addition, let  $\vartheta^*$  be the optimal solution of SCP (4.6). By considering  $x_1, x_2 \in \Phi_{\eta_x/2}(\hat{x})$  and picking samples  $x_l, x_{\bar{l}}$  from cells  $\Phi_{\hat{\eta}_x/2}(x_l), \Phi_{\hat{\eta}_x/2}(x_{\bar{l}}) \subset \Phi_{\eta_x/2}(\hat{x})$ , and  $w'_1, w'_2 \in \Phi_{\eta_w/2}(\hat{w})$ , one gets

$$\begin{aligned} &\|\beta(\vartheta^*, x_1, x_2, w_1, w_2) - \beta(\vartheta^*, x_l, x_{\bar{l}}, w'_1, w'_2)\| \\ &\leq \|f(x_1, \hat{u}, w_1) - f(x_l, \hat{u}, w'_1)\| + \|\vartheta_1(\hat{x}, \hat{u}, \hat{w})\| \|x_1 - x_l\| \\ &\quad + \|f(x_2, \hat{u}, w_2) - f(x_{\bar{l}}, \hat{u}, w'_2)\| + \|\vartheta_1(\hat{x}, \hat{u}, \hat{w})\| \|x_2 - x_{\bar{l}}\| \\ &\quad \text{(using Lemma 4.5)} \\ &\leq 2\mathcal{L}_x(\|x_1 - x_l\| + \|x_2 - x_{\bar{l}}\|) + \mathcal{L}_w(\|w_1 - w'_1\| + \|w_2 - w'_2\|) \\ &\leq 2\mathcal{L}_x\|\hat{\eta}_x\| + \mathcal{L}_w\|\eta_w\|. \end{aligned}$$

The above inequality implies that

$$(4.8) \quad \beta(\vartheta^*, x_1, x_2, w_1, w_2) \leq \beta(\vartheta^*, x_l, x_{\bar{l}}, w'_1, w'_2) + \varrho,$$

where  $\varrho := 2\mathcal{L}_x\hat{\eta}_x + \mathcal{L}_w\|\eta_w\|\mathbf{1}_{\dim(\mathcal{X})}$ . Therefore, within any cell  $\Phi_{\eta_x/2}(\hat{x})$ , (4.8) implies that any optimal solution of SCP (4.6) is always feasible for RCP (4.5). In particular, any feasible solution of (4.6) results in a growth bound  $\kappa_\vartheta$  of the form (4.2) that satisfies inequality (4.1), which concludes the proof.  $\square$

We propose Algorithm 1 to illustrate the required procedures in Theorem 4.6 for the data-driven construction of finite abstractions of subsystems. We present a visual representation of the transition function  $\hat{f}(\hat{x}, \hat{u}, \hat{w})$  for a finite abstraction of a subsystem in Fig. 2.

---

**Algorithm 1** Construction of Subsystems Abstractions (SA)

---

**Require:**  $SA(\mathcal{X}, U, \mathcal{U}, \eta_x, \eta_u, \eta_w)$

- 1: Construct:  $\hat{\mathcal{X}} = [\mathcal{X}]_{\eta_x}$ ,  $\hat{U} = [U]_{\eta_u}$ ,  $\hat{\mathcal{U}} = [\mathcal{U}]_{\eta_w}$
- 2: **for each**  $(\hat{x}, \hat{u}, \hat{w}) \in (\hat{\mathcal{X}}, \hat{U}, \hat{\mathcal{U}})$  **do**
- 3:   Initiate:  $\hat{f}(\hat{x}, \hat{u}, \hat{w}) = \emptyset$ ,  $\gamma = \mathbf{0}$
- 4:   Obtain  $c = f(\hat{x}, \hat{u}, \hat{w})$  by simulating dt-CS (2.4) from the initial condition  $\hat{x}$  under the input pair  $(\hat{u}, \hat{w})$
- 5:   Compute  $\varrho \in \mathbb{R}_{\geq 0}^{\dim(\mathcal{X})}$  as in (4.7)
- 6:   As outlined in Theorem 4.6, generate  $[\Phi_{\eta_x/2}(\hat{x})]_{\hat{\eta}_x}$  and select  $\mathcal{N}_C$  sampled data points  $(x_l, \hat{u}, \hat{w}, x'_l)$  from it.
- 7:   Obtain the optimal value  $\vartheta^*(\hat{x}, \hat{u}, \hat{w})$  for the SCP in (4.6)
- 8:   Update  $\gamma = \kappa_{\vartheta^*}(\eta_x, \hat{x}, \hat{u}, \hat{w})$
- 9:    $\hat{f}(\hat{x}, \hat{u}, \hat{w}) = \{\hat{x}' \in \hat{\mathcal{X}} \mid \Phi_{\eta_x/2}(\hat{x}') \cap \Phi_\gamma(c) \neq \emptyset\} \cup \hat{f}(\hat{x}, \hat{u}, \hat{w})$
- 10: **end for**

**Ensure:**  $\hat{\Xi} = (\hat{\mathcal{X}}, \hat{U}, \hat{\mathcal{U}}, \hat{f})$

---



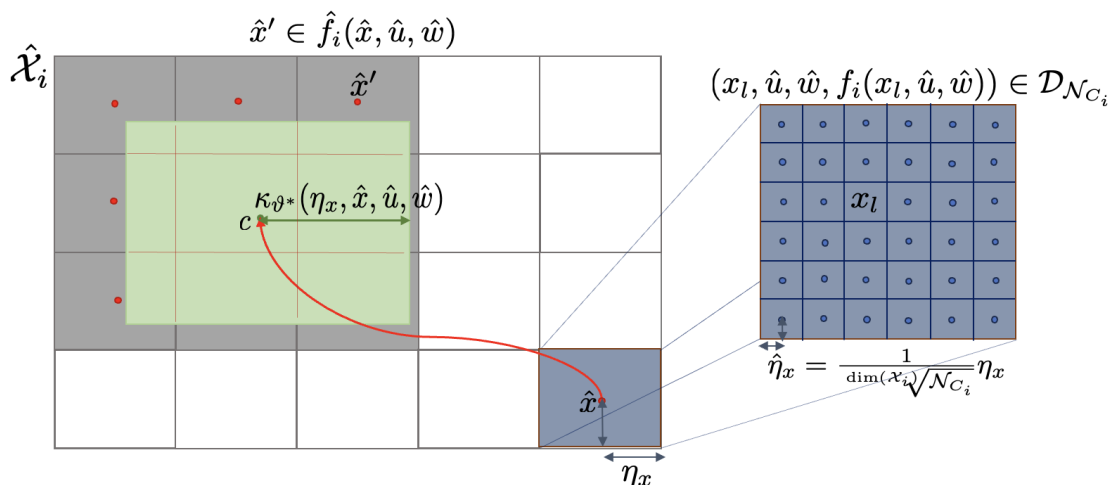


FIGURE 2. A 2-dimensional depiction of a finite abstraction for a subsystem, constructed using Algorithm 1.

*Remark 4.7.* Utilizing Theorem 4.6 across all partition sets enables the establishment of a set membership relation  $\preceq_{\mathcal{Q}}$  (cf. Theorem 4.4) between a concrete subsystem  $\Xi$  and its data-driven finite abstraction  $\widehat{\Xi}$ . This abstraction is constructed by solving SCP (4.6) over the grid cells.

**4.2. Finite Abstractions for Interconnections.** Upon obtaining the subsystem abstractions, as in the preceding subsection, we proceed to the second phase of addressing Problem 3.4. This phase involves creating a symbolic representation of the interconnection. The construction of arbitrary interconnections can, in the worst-case scenario, exhibit exponential complexity with respect to the number of subsystems  $N$ . To mitigate this, we introduce supplementary variables that account for intermediate computations within the abstraction construction. This not only introduces sparsity but also reduces the computational load associated with the abstraction process.

Consider an interconnection  $\mathcal{I} = (\mathcal{X}^{\mathcal{I}}, \mathcal{U}^{\mathcal{I}}, \mathcal{M})$  as in Definition 3.1. Note that the interconnection map  $\mathcal{M}$  (3.1) is an unknown nonlinear map. However, we have access to the input-output data points as in  $\mathcal{D}_{\mathcal{N}_I}$ . Our goal is to derive a linear approximation  $\overline{\mathcal{M}}$  of  $\mathcal{M}$ , serving as the basis for constructing an abstraction  $\widehat{\mathcal{I}}$ . To do so, we first frame the search for the linear estimate as a regression problem. The estimator is subject to regularization via an  $\ell_1$ -norm penalty term, promoting sparsity. This is detailed as follows:

$$(4.9) \quad \arg \min_{\overline{\mathcal{M}}} \left\{ \|\Omega - \mathbb{X}\overline{\mathcal{M}}\|_2^2 + \alpha \|\overline{\mathcal{M}}^\top\|_1 \right\},$$

where for data points  $\{(x_l, w_l)\}_{l=1}^{\overline{\mathcal{N}}_I}$  in  $\mathcal{D}_{\mathcal{N}_I}$ ,  $\Omega$  and  $\mathbb{X}$  are the stack of  $\{w_l\}$  and  $\{x_l\}$ , respectively, with  $l \in [1; \overline{\mathcal{N}}_I]$  such that  $\overline{\mathcal{N}}_I < \mathcal{N}_I$ . Note that it is not necessary to utilize all data points in  $\mathcal{D}_{\mathcal{N}_I}$  to formulate equation (4.9) for estimating  $\mathcal{M}$ . Instead, we rely on only a subset of  $\mathcal{D}_{\mathcal{N}_I}$ . Note that for a network comprising of  $N$  interconnected subsystems governed by a linear interconnection map, one can readily verify that acquiring  $\dim(\mathcal{U}^{\mathcal{I}}) \times \dim(\mathcal{X}^{\mathcal{I}})$  input-output data points of the interconnection map is sufficient for accurately estimating the map (cf. Subsection 5.2). Note that  $\alpha > 0$  denotes the regularization parameter and  $\overline{\mathcal{M}} \in \mathbb{R}^{\dim(\mathcal{U}^{\mathcal{I}}) \times \dim(\mathcal{X}^{\mathcal{I}})}$ . The term  $\alpha \|\overline{\mathcal{M}}^\top\|_1$  in (4.9) enforces sparsity on  $\overline{\mathcal{M}}$  row by row, thereby reducing the computational effort needed for constructing the overall abstraction. However, to accomplish the desired sparsity on  $\overline{\mathcal{M}}$  from (4.9), an appropriate value must be selected for parameter  $\alpha$ . One may opt for the process of tuning the penalty term through cross-validation [Lju98], involving systematically assessing a range of penalty values on validation data.

It is important to note that the regression formulation in (4.9) is numerically solvable, guaranteeing the existence of a solution for the specified optimization problem. Consequently, given  $x_l \in \mathcal{X}^{\mathcal{I}}$ , the actual value

$w_l = \mathcal{M}(x_l) \in \mathcal{U}^{\mathcal{I}}$  is estimated by  $\overline{\mathcal{M}}x_l$ , accounting for a residual error. We present the next lemma, which plays a crucial role in the process of constructing an abstraction for an interconnection  $\mathcal{I}$ .

**Lemma 4.8.** *Consider a data point  $(x_l, w_l) \in \mathcal{D}_{N_l}$  and a neighbourhood  $\Phi_{\rho_x}(x_l) \subset \mathcal{X}^{\mathcal{I}}$  of  $x_l$ , where  $\rho_x \in \mathbb{R}_{>0}^{\dim(\mathcal{X}^{\mathcal{I}})}$ . Then, for any  $x' \in \Phi_{\rho_x}(x_l)$ , there exists  $\hat{\varepsilon}(\rho_x, w_l, x') \in \mathbb{R}_{>0}$  such that*

$$\mathcal{M}(x') \in \overline{\mathcal{M}}x' \oplus [-\hat{\varepsilon}(\rho_x, w_l, x')\mathbf{1}_{\dim(\mathcal{U}^{\mathcal{I}})}, \hat{\varepsilon}(\rho_x, w_l, x')\mathbf{1}_{\dim(\mathcal{U}^{\mathcal{I}})}].$$

*Proof.* Consider any  $x' \in \mathcal{X}^{\mathcal{I}}$  where  $|x_l - x'| \leq \rho_x$ . Then the following inequalities hold:

$$\begin{aligned} \|\mathcal{M}(x') - \overline{\mathcal{M}}x'\| &\leq \|\mathcal{M}(x') - \mathcal{M}(x_l)\| + \|\mathcal{M}(x_l) - \overline{\mathcal{M}}x'\| \\ &\leq \mathcal{L}_{\mathcal{M}}\|x' - x_l\| + \|w_l - \overline{\mathcal{M}}x'\| \\ &\leq \mathcal{L}_{\mathcal{M}}\|\rho_x\| + \|w_l - \overline{\mathcal{M}}x'\|. \end{aligned}$$

Now, let

$$(4.10) \quad \hat{\varepsilon}(\rho_x, w_l, x') := \mathcal{L}_{\mathcal{M}}\|\rho_x\| + \|w_l - \overline{\mathcal{M}}x'\|.$$

Therefore, for any  $x' \in \Phi_{\rho_x}(x_l)$ ,  $\|\mathcal{M}(x') - \overline{\mathcal{M}}x'\| \leq \hat{\varepsilon}(\rho_x, w_l, x')$ , which concludes the proof.  $\square$

Observe that the parameter  $\hat{\varepsilon}(\rho_x, w_l, x')$  depends on the data point  $(x_l, w_l) \in \mathcal{D}_{N_l}$ , along with the distance  $\rho_x \in \mathbb{R}_{>0}^{\dim(\mathcal{X}^{\mathcal{I}})}$  of the neighborhood around  $x_l$ , considering the particular point  $x'$  within the neighborhood. Using  $\overline{\mathcal{M}}$  to derive an over-approximation of  $\mathcal{M}(x')$  in accordance with Lemma 4.8 implies creating an interconnection abstraction in a monolithic fashion. This approach necessitates a brute-force traversal of the set  $\mathcal{X}^{\mathcal{I}}$ . The computational complexity of this brute-force exploration experiences an exponential increase with the number of subsystems  $N$ . Hence, we illustrate how integrating additional variables, representing intermediate computations through the decomposition of  $\overline{\mathcal{M}}$ , can reduce the runtime of the interconnection abstraction. This reduction occurs because the brute-force traversal is conducted over lower-dimensional subspaces, consequently alleviating the computational burden associated with the abstraction process.

Consider a  $x \in \Phi_{\rho_x}(x_l)$  according to Lemma 4.8. Let

$$(4.11) \quad w = \overline{\mathcal{M}}x + \hat{\varepsilon}(\rho_x, w_l, x)\mathbf{1}_{\dim(\mathcal{U}^{\mathcal{I}})}.$$

We proceed by transforming the sparse matrix  $\overline{\mathcal{M}} \in \mathbb{R}^{\dim(\mathcal{U}^{\mathcal{I}}) \times \dim(\mathcal{X}^{\mathcal{I}})}$  into a weighted directed acyclic graph (WDAG)  $G = (V, E)$  such that the following hold:

- The sets of vertices  $w_I = \{w_1, \dots, w_N\}$  and  $x_I = \{x_1, \dots, x_N\}$  satisfy  $w_I \cup x_I \subseteq V$ .
- The edge function  $e : x_I \times w_I \rightarrow \mathbb{R}_{>0} \cup \{\text{invalid}\}$  is defined as:

$$(4.12) \quad e(x_j, w_j) := \begin{cases} \text{invalid} & \text{if } \overline{\mathcal{M}}_{ij} = 0 \\ \overline{\mathcal{M}}_{ij} & \text{otherwise.} \end{cases}$$

- The set of edges  $E = \{(v, v') \in V \times V \mid e(v, v') \text{ is not invalid}\}$ .

We emphasize that an edge  $(v, v') \in V \times V$  is considered invalid if it is not included in the graph  $G$ , meaning  $(v, v') \notin E$ . Additionally, for any vertex  $v \in V$ , we define the set  $\mathcal{D}(v) := \{v' \mid e(v', v) \text{ is not invalid}\}$ . Consequently, the indegree of  $v$ , denoted as  $\text{deg}(v)$ , is defined as  $\mathcal{C}_d(\mathcal{D}(v))$ . We proceed to decompose the matrix  $\overline{\mathcal{M}}$  by leveraging its corresponding WDAG, applying the procedures outlined in Algorithm 2. It is important to mention that Algorithm 2 takes a user-specified hyperparameter  $\sigma \in \mathbb{N}_{\geq 1}$  as an input, which governs the number of nodes in the ultimate layer of the WDAG. In order to avoid possible computational challenges (refer to Lines 4 to 8 of Algorithm 3), it is recommended that  $\sigma$  is limited to a maximum value of 4.

In Fig. 3 (top), we provide an example of a WDAG of  $\overline{\mathcal{M}} \in \mathbb{R}_{>0}^{1 \times 8}$  with a uniform weight of 1/8 on each edge. This example is further explained in Subsection 5.2. The graph features a shared node  $w$  such that

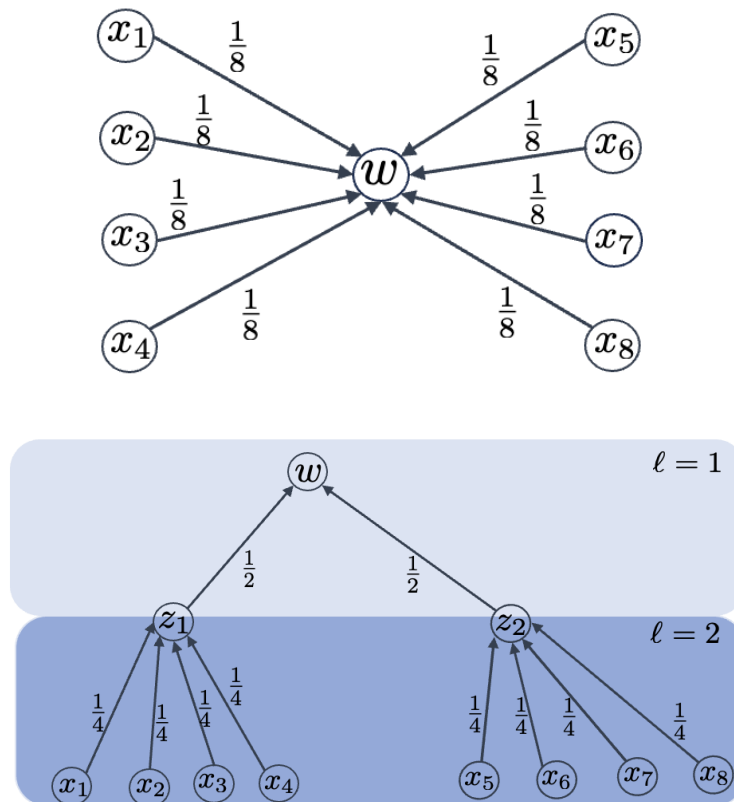


FIGURE 3. An illustration of a WDAG with the application of Algorithm 2 where  $\sigma = 4$ .

$\deg(w) = 8$ . Applying Algorithm 2 with  $\sigma = 4$  yields the lower part of the figure. Two intermediate variables  $\{z_1, z_2\}$  have been introduced to the graph, effectively decomposing  $\overline{\mathcal{M}} \in \mathbb{R}_{>0}^{1 \times 8}$  to  $M_1 \in \mathbb{R}_{>0}^{1 \times 2}$  and  $M_2 \in \mathbb{R}_{>0}^{1 \times 4}$ .

In the abstraction process, instead of over-approximating  $\overline{\mathcal{M}}\hat{x}$  for a  $\hat{x} \in \mathcal{X}^{\mathcal{I}} \subset \mathbb{R}_{\geq 0}^8$ , we leverage the decomposition of  $\overline{\mathcal{M}}$  to compute the over-approximation. Thus, in this example, (4.11) which involves computations in  $\mathbb{R}^8$  is decomposed into computations in  $\mathbb{R}^2$  and  $\mathbb{R}^4$ . Consequently, the set  $\overline{\mathcal{M}}\hat{x} \oplus [-\hat{\varepsilon}(\rho_x, w_l, \hat{x}), \hat{\varepsilon}(\rho_x, w_l, \hat{x})]$  is over-approximated as  $\{\prod_{i=1}^2 (M_i x_i \oplus [-\hat{\varepsilon}(\rho_x, w_l, \hat{x}), \hat{\varepsilon}(\rho_x, w_l, \hat{x})]) \mid \hat{x} = [x_1; x_2]\}$ , and grids of dimension 2 and 4 are availed instead of dimension 8 for the abstraction.

Furthermore, we propose Algorithm 3 to outline the process of constructing the interconnection abstraction. Note that in line 5 of Algorithm 3, the computational burden associated with traversing a higher-dimensional space  $\mathcal{X}^{\hat{\mathcal{I}}}$  is mitigated through the decomposition of  $\overline{\mathcal{M}}$  in line 4. This decomposition is utilized in the construction of the over-approximation, as outlined in line 8. Additionally, we formally establish that the interconnection created by using Algorithm 3 is a correct abstraction of the concrete *unknown* interconnection.

**Theorem 4.9.** *Consider an interconnection  $\mathcal{I} = (\mathcal{X}^{\mathcal{I}}, \mathcal{U}^{\mathcal{I}}, \mathcal{M})$  where the map  $\mathcal{M}$  is unknown. Let  $\rho_x \in \mathbb{R}_{>0}^{\dim(\mathcal{X}^{\mathcal{I}})}$  and  $\rho_w \in \mathbb{R}_{>0}^{\dim(\mathcal{U}^{\mathcal{I}})}$  be discretization parameters utilized to form symbolic sets  $\mathcal{X}^{\hat{\mathcal{I}}} = [\mathcal{X}^{\mathcal{I}}]_{\rho_x}$  and  $\mathcal{U}^{\hat{\mathcal{I}}} = [\mathcal{U}^{\mathcal{I}}]_{\rho_w}$ . Suppose  $\hat{\mathcal{I}} = (\mathcal{X}^{\hat{\mathcal{I}}}, \mathcal{U}^{\hat{\mathcal{I}}}, \hat{\mathcal{M}})$  is constructed using Algorithm 3. Then  $\hat{\mathcal{I}}$  is an abstraction of  $\mathcal{I}$  as in Definition 3.1.*

**Algorithm 2** Matrix Decomposition (*MDec*)**Require:**  $MDec(\overline{\mathcal{M}}, \sigma)$ 

- 1: Generate the corresponding WDAG  $G = (V = w_I \cup x_I, E)$
  - 2: Initiate matrix set  $MS = \emptyset$
  - 3: **while**  $deg(v) > \sigma \ \forall v \in V$  **do**
  - 4:   Initiate set of auxilliary variables  $Z_\ell = \emptyset$  with layer  $\ell = 1$
  - 5:   Pick  $d \in [1; \sigma]$  and create vertices  $z_i$  where  $1 \leq i \leq d$
  - 6:   Let  $p := C_d(w_I)$  and create matrix  $M_\ell \in \mathbb{R}_{>0}^{p \times d}$  with entries  $e(z_i, v)$  set to null  $\forall v \in w_I$  and  $1 \leq i \leq d$
  - 7:   **for each**  $v \in w_I$  **do**
  - 8:     **if**  $deg(v) \leq \sigma$  **then**
  - 9:       Continue
  - 10:    **else**
  - 11:     Set  $e(z_i, v) := 1/d$  and let  $d' := C_d(\mathcal{D}(v))$
  - 12:      $D := [v'_1; v'_2; \dots; v'_d]$  where  $v'_j \in \mathcal{D}(v) \ \forall j \in [1; d']$
  - 13:     Set  $e(D[j], z_i) := e(D[j], v)/e(z_i, v)$  until all vertices  $D[j]$  has been connected to a vertex  $z_i$  where  $1 \leq j \leq d'$  and  $1 \leq i \leq d$
  - 14:      $E = E \setminus \{(v', v) \in V \times V \mid v' \in \mathcal{D}(v)\}$
  - 15:      $Z_\ell = Z_\ell \cup \{z_i \mid 1 \leq i \leq d\}$
  - 16:    **end if**
  - 17:   **end for**
  - 18:    $w_I = Z_\ell$ ,  $\ell = \ell + 1$  and  $MS = MS \cup \{M_\ell\}$
  - 19: **end while**
- Ensure:**  $MS$

**Algorithm 3** Construction of Interconnection Abstraction (*IA*)**Require:**  $IA(\mathcal{X}^{\mathcal{I}}, \mathcal{U}^{\mathcal{I}}, \rho_x, \rho_w)$ 

- 1: Initiate:  $\mathcal{X}^{\hat{\mathcal{I}}} = [\mathcal{X}^{\mathcal{I}}]_{\rho_x}$  and  $\mathcal{U}^{\hat{\mathcal{I}}} = [\mathcal{U}^{\mathcal{I}}]_{\rho_w}$
  - 2: Collect data in set  $\mathcal{D}_{\mathcal{N}_I} = \{(x_l, w_l) \in \mathcal{X}^{\mathcal{I}} \times \mathcal{U}^{\mathcal{I}} \mid x_l \in \Phi_{\rho_x}(\hat{x}) \text{ where } \hat{x} \in \mathcal{X}^{\hat{\mathcal{I}}}, l = 1, \dots, \mathcal{N}_I\}$  and select appropriate value for  $\sigma$
  - 3: Using  $\mathcal{N}_I < \mathcal{N}_I$  data points, solve (4.9) to obtain  $\overline{\mathcal{M}}$
  - 4: Obtain  $MS := MDec(\overline{\mathcal{M}}, \sigma)$  and let  $q := C_d(MS)$
  - 5: **for each**  $\hat{x} \in \mathcal{X}^{\hat{\mathcal{I}}}$  **do**
  - 6:   Initiate  $\hat{\mathcal{M}}(\hat{x}) = \emptyset$  and compute  $\hat{\varepsilon} := \hat{\varepsilon}(\rho_x, w_l, \hat{x}) > 0$  as in (4.10)
  - 7:   Construct lower dimensional grids  $[\mathcal{X}^{\mathcal{I}}]_{\|\rho_x\| \mathbf{1}_i}$  where  $i \in [1; q]$
  - 8:    $B := \{\prod_{i=1}^q (M_i x_i \oplus [-\hat{\varepsilon} \mathbf{1}_i, \hat{\varepsilon} \mathbf{1}_i]) \mid \hat{x} = [x_1; \dots; x_q]\}$
  - 9:    $\hat{\mathcal{M}}(\hat{x}) = \{\hat{w}' \in \mathcal{U}^{\hat{\mathcal{I}}} \mid \Phi_{\rho_w}(\hat{w}') \cap B \neq \emptyset\} \cup \hat{\mathcal{M}}(\hat{x})$
  - 10: **end for**
- Ensure:**  $\hat{\mathcal{I}} = (\mathcal{X}^{\hat{\mathcal{I}}}, \mathcal{U}^{\hat{\mathcal{I}}}, \hat{\mathcal{M}})$

*Proof.* Suppose  $(x, \hat{x}) \in \mathcal{X}^{\mathcal{I}} \times \mathcal{X}^{\hat{\mathcal{I}}}$  such that  $|x - \hat{x}| \leq \rho_x$  and  $w = \mathcal{M}(x)$ . Line 1 of Algorithm 3 implies that there exists  $\hat{w} \in \mathcal{U}^{\hat{\mathcal{I}}}$  such that  $w \in \Phi_{\rho_w}(\hat{w})$ . Upon solving (4.9), we obtain an approximation  $\overline{\mathcal{M}}$  of  $\mathcal{M}$ . Then Lemma 4.8 implies that there exists  $\hat{\varepsilon} = \hat{\varepsilon}(\rho_x, w_l, \hat{x}) > 0$  such that  $|\mathcal{M}(x) - \overline{\mathcal{M}}x| \leq \hat{\varepsilon} \mathbf{1}_{\dim(\mathcal{U}^{\mathcal{I}})}$ . Hence,  $w \in \Phi_{\hat{\varepsilon} \mathbf{1}_{\dim(\mathcal{U}^{\mathcal{I}})}}(\overline{\mathcal{M}}x)$ , which implies that  $\Phi_{\rho_w}(\hat{w}) \cap \Phi_{\hat{\varepsilon} \mathbf{1}_{\dim(\mathcal{U}^{\mathcal{I}})}}(\overline{\mathcal{M}}x) \neq \emptyset$ . Therefore, line 9 of Algorithm 3 yields that  $\hat{w} \in \hat{\mathcal{M}}(\hat{x})$ , which satisfies the condition outlined in Definition 3.3, concluding the proof.  $\square$

**4.3. Compositional Construction of Abstraction.** Here, we begin by presenting a compositional result that establishes a feedback refinement relation between an interconnected abstraction and the concrete

interconnected dt-CS. This result leverages the feedback refinement relations from individual concrete subsystems to their respective abstractions. Subsequently, we outline a scheme for integrating the subsystem abstraction and the interconnection abstraction in a compositional manner. Suppose we have  $N$  subsystems  $\Xi_i = (\mathcal{X}_i, U_i, \mathcal{U}_i, f_i)$ , accompanied by their finite abstractions  $\hat{\Xi}_i = (\hat{\mathcal{X}}_i, \hat{U}_i, \hat{\mathcal{U}}_i, \hat{f}_i)$ , and feedback refinement relations  $\mathcal{Q}_i$  from  $\Xi_i$  to  $\hat{\Xi}_i$ , where  $i \in [1; N]$  (cf. Theorem 4.4). We present the following theorem, which establishes a feedback refinement relation between a concrete interconnected dt-CS and the data-driven finite abstractions of the subsystems that have been composed together.

**Theorem 4.10.** *Consider an interconnected dt-CS  $\Xi = \mathcal{I}(\Xi_1, \dots, \Xi_N)$ , consisting of  $N \in \mathbb{N}_{\geq 1}$  subsystems  $\Xi_i$  and an interconnection  $\mathcal{I} = (\mathcal{X}^{\mathcal{I}}, \mathcal{U}^{\mathcal{I}}, \mathcal{M})$ . Let each subsystem  $\Xi_i$  admits a data-driven abstraction  $\hat{\Xi}_i$  constructed as in Algorithm 1 such that  $\Xi_i \preceq_{\mathcal{Q}_i} \hat{\Xi}_i \forall i \in [1; N]$  (e.g. as in Theorem 4.4). Additionally, assume that  $\hat{\mathcal{I}} = (\hat{\mathcal{X}}^{\hat{\mathcal{I}}}, \hat{\mathcal{U}}^{\hat{\mathcal{I}}}, \hat{\mathcal{M}})$  is an abstraction of  $\mathcal{I}$  constructed as in Algorithm 3. Consider a relation  $Q \subseteq \mathcal{X}^{\mathcal{I}} \times \hat{\mathcal{X}}^{\hat{\mathcal{I}}}$  such that  $\forall (x, \hat{x}) \in Q$  where  $x = [x_1; \dots; x_N]$  and  $\hat{x} = [\hat{x}_1; \dots; \hat{x}_N]$ ,  $(x_i, \hat{x}_i) \in \mathcal{Q}_i \forall i \in [1; N]$ . Then relation  $Q$  is a feedback refinement relation from  $\Xi$  to  $\hat{\mathcal{I}}(\hat{\Xi}_1, \dots, \hat{\Xi}_N)$ .*

*Proof.* Given that  $\Xi_i \preceq_{\mathcal{Q}_i} \hat{\Xi}_i, \forall i \in [1; N]$ , let  $\hat{u} := [\hat{u}_1; \dots; \hat{u}_N] \in U_{\hat{\mathcal{I}}(\hat{\Xi}_1, \dots, \hat{\Xi}_N)}(\hat{x})$  where  $\hat{x} = [\hat{x}_1; \dots; \hat{x}_N] \in \hat{\mathcal{X}}^{\hat{\mathcal{I}}}$ . Thus,  $\exists \hat{x}' \in \hat{f}(\hat{x}, \hat{u})$ , and by (3.2)  $\hat{f}(\hat{x}, \hat{u}) := \{[\hat{x}'_1; \dots; \hat{x}'_N] \mid \hat{x}'_i \in \hat{f}_i(\hat{x}_i, \hat{u}_i, \hat{w}_i) \forall i \in [1; N]\}$  where  $\forall w := [w_1; \dots; w_N] = \mathcal{M}([x_1; \dots; x_N]) \exists \hat{w} := [\hat{w}_1; \dots; \hat{w}_N] \in \hat{\mathcal{M}}(\hat{x})$  and there is a relation  $\tilde{\mathcal{R}} \subseteq \mathcal{U}^{\mathcal{I}} \times \hat{\mathcal{U}}^{\hat{\mathcal{I}}}$  such that  $(w, \hat{w}) \in \tilde{\mathcal{R}}$ . Suppose that  $(x, \hat{x}) \in Q$  where  $x = [x_1; \dots; x_N] \in \mathcal{X}^{\mathcal{I}}$  and  $(x_i, \hat{x}_i) \in \mathcal{Q}_i, \forall i \in [1; N]$ . Thus,  $\hat{u}_i \in U_{\hat{\Xi}_i}(\hat{x}_i, \hat{w}_i) \implies \mathcal{Q}_i(f_i(x_i, \hat{u}_i, w_i)) \subseteq \hat{f}_i(\hat{x}_i, \hat{u}_i, \hat{w}_i) \forall i \in [1; N]$ . Since  $\hat{x}_i \in \hat{f}_i(\hat{x}_i, \hat{u}_i, \hat{w}_i), \forall i \in [1; N]$ , and by Definition 2.3,  $\exists w_i \in \mathcal{U}_i$  and  $x'_i \in \mathcal{X}_i$  such that  $x'_i = f_i(x_i, \hat{u}_i, w_i) \forall i \in [1; N]$ . Therefore,  $x' = f(x, \hat{u}) := [x'_1; \dots; x'_N] \mid x'_i = f_i(x_i, \hat{u}_i, w_i) \forall i \in [1; N]$ , and as a result,  $\hat{u} \in U_{\Xi}(x)$ , which implies that  $U_{\hat{\mathcal{I}}(\hat{\Xi}_1, \dots, \hat{\Xi}_N)}(\hat{x}) \subseteq U_{\Xi}(x)$ . Now, suppose that  $\hat{x}' \in Q(f(x, \hat{u}))$ , then  $\hat{x}' \in \mathcal{Q}_i(f_i(x_i, \hat{u}_i, w_i)) \forall i \in [1; N]$ . This implies  $\hat{x}'_i \in \hat{f}_i(\hat{x}_i, \hat{u}_i, \hat{w}_i), \forall i \in [1; N]$ , which implies that  $\hat{x}' \in \hat{f}(\hat{x}, \hat{u})$ . Hence,  $Q(f(x, u)) \subseteq \hat{f}(\hat{x}, \hat{u})$ , and the conditions in Definition 2.4 are satisfied, concluding the proof.  $\square$

*Remark 4.11.* Theorem 4.10 enables the construction of a finite abstraction of a network of subsystems by utilizing finite abstractions of individual subsystems, as depicted in Fig. 1.

The abstractions derived for both the subsystems and the interconnection via Algorithm 1 and 3, respectively, are encoded using binary decision diagrams (BDD) [Bry86]. This selection of the data structure efficiently encodes the abstractions as Boolean-valued functions. Hence, each subsystem abstraction have an encoding  $(\hat{x}_i, \hat{u}_i, \hat{w}_i, \hat{x}'_i) - \hat{f}_i \rightarrow \{\mathbf{true}, \mathbf{false}\}, \forall i \in [1; N]$ . Similarly, the interconnection abstraction is encoded as  $(\hat{x}, \hat{w}') - \hat{\mathcal{M}} \rightarrow \{\mathbf{true}, \mathbf{false}\}$ . Consequently, we utilize this representation of abstractions to combine and interconnect the subsystem abstractions through Boolean conjunctions, taking into account all conditions as delineated in Definition 3.2. Thus, we outline the complete solution to Problem 3.4 in Algorithm 4.

---

#### Algorithm 4 Data-Driven Compositional Abstraction (CA)

---

**Require:**  $CA(\mathcal{I}(\Xi_1, \dots, \Xi_N), \{\eta_{x_i}, \eta_{w_i}, \eta_{w_i}\}_{i=1}^N, \rho_x, \rho_w)$

- 1: Initiate  $Abs = \mathbf{true}$
- 2: **for each**  $i \in [1; N]$  **do**
- 3:    $Abs' = SA(\Xi_i, \eta_{x_i}, \eta_{w_i})$
- 4:    $Abs = Abs \wedge Abs'$
- 5: **end for**
- 6:  $Abs = Abs \wedge IA(\mathcal{I}(\Xi_1, \dots, \Xi_N), \rho_x, \rho_w)$

**Ensure:**  $Abs$

---

## 5. CASE STUDIES

In this section, we demonstrate the efficacy of our proposed approaches by applying them to two numerical benchmarks models, which were borrowed from [KAZ18]. However, we have assumed that these models and their interconnection maps are unknown in applying our approach. The abstractions for both subsystems and the interconnection are symbolically represented using Boolean functions, which have been implemented with the CUDD toolbox [Som97]. All implementations for the construction of the data-driven finite abstractions have been carried out in a modified version of the toolbox SCOTS [RZ16], using a 64-bit MacBook Pro with 64GB RAM (3.2 GHz).

**5.1. Experimental Evaluation for Scalability.** We now present an example designed to illustrate the scalability of the interconnection decomposition introduced in Algorithm 2 for a range of  $N$  subsystems. Consider a collection of  $N$  scalar subsystems  $\Xi_i = (\mathcal{X}_i, U_i, \mathcal{U}, f_i)$  where  $\mathcal{X}_i = [0, 32]$ ,  $U_i = [0, 7]$ ,  $\mathcal{U} = [0, 32]$  and

$$(5.1) \quad \begin{aligned} x_i(k+1) &= f_i(x_i(k), u_i(k), w(k)) \\ &= \min(0.75(x_i(k) + u_i(k)), w(k) + 1, 32), \end{aligned}$$

such that there is a single variable  $w(k) \in \mathcal{U}$  shared amongst all subsystems, *i.e.*,

$$(5.2) \quad w(k) = \max(x_1(k), \dots, x_N(k)).$$

It is evident from models in (5.1) and (5.2) that a one-time-step evolution of any subsystem depends on the previous state of other subsystems. Utilizing these models, we generate the data sets  $\mathcal{D}_{\mathcal{N}_{C_i}}$  and  $\mathcal{D}_{\mathcal{N}_I}$ , respectively. Furthermore, we estimate the Lipschitz constants as  $\mathcal{L}_{x_i} = \mathcal{L}_{w_i} = \mathcal{L}_{\mathcal{M}} = 1.0$  (cf. Remark 4.1 and [SLSZ24, Lemma A.2.]). In Algorithm 1, we employed  $\mathcal{N}_{C_i} = 150$  samples. The abstract sets  $\hat{\mathcal{X}}_i$  and  $\hat{\mathcal{U}}$  were constructed using grid parameters  $\eta_{x_i} = \eta_w = 1$  for all  $i \in [1; N]$ , while the external input grid was defined as  $\hat{U}_i = [U_i]_1$ . To construct the interconnection abstraction  $\hat{\mathcal{T}} = (\prod_{i=1}^N \hat{\mathcal{X}}_i, \hat{\mathcal{U}}, \hat{\mathcal{M}})$ , we solved (4.9) using  $\mathcal{N}_I = 200$  input-output data points from (5.2). After obtaining  $\overline{\mathcal{M}} \in \mathbb{R}^N$ , a decomposition  $M_1 := \frac{1}{N} \overline{\mathcal{M}} \cdot [\mathbf{1}_N \ \mathbf{1}_N]$  follows from Algorithm 2 to introduce intermediate variables as follows:

$$(5.3) \quad \begin{aligned} z_1 &= M_1 \cdot [x_1; x_2]^\top, \\ z_i &= M_1 \cdot [z_{i-1}; x_{i+1}]^\top, \quad \forall i \in [2; N-2], \\ w &= M_1 \cdot [z_{N-2}; x_N]^\top, \end{aligned}$$

where the intermediate variables  $z_j$ ,  $\forall j \in [1; N-2]$ , belongs to  $\hat{\mathcal{X}}_i$ . Fig. 4 reports the runtimes required to construct both the  $N$  abstract subsystems and the abstract interconnection, as well as their composition.

**5.2. Consensus-Driven Network of Logistic Systems.** We consider a network consisting of  $N$  subsystems, each characterized by state sets  $\mathcal{X}_i = [0, 32]$  and input sets  $U_i = [-2, 2]$ , where  $i \in [1; N]$ . Additionally, the subsystems share an internal input  $\mathcal{U} = [0, 32]$ . The dynamics governing each subsystem  $\Xi_i$  are defined as follows:

$$(5.4) \quad \begin{aligned} x_i(k+1) &= f_i(x_i(k), u_i(k), w_i(k)) \\ &= \text{GLOG}_{[a,b]}(x_i(k) + u_i(k) + 0.1(x_i(k) - w(k))), \end{aligned}$$

where  $\text{GLOG}_{[a,b]}(\cdot)$  represents a generalized logistic function over  $[a, b] \subseteq [0, 32]$ , producing output values within the range  $[0, 32]$ . Mathematically, this function is defined as:

$$\text{GLOG}_{[a,b]}(x) := \frac{32}{1 + e^{-0.2(x - \frac{b+a}{2})}}.$$

The function  $\text{GLOG}_{[a,b]}(\cdot)$  is characterized by its sigmoid shape and ensures that the output is bounded within the specified range. The interconnected system must satisfy a persistent objective, ensuring it reaches and

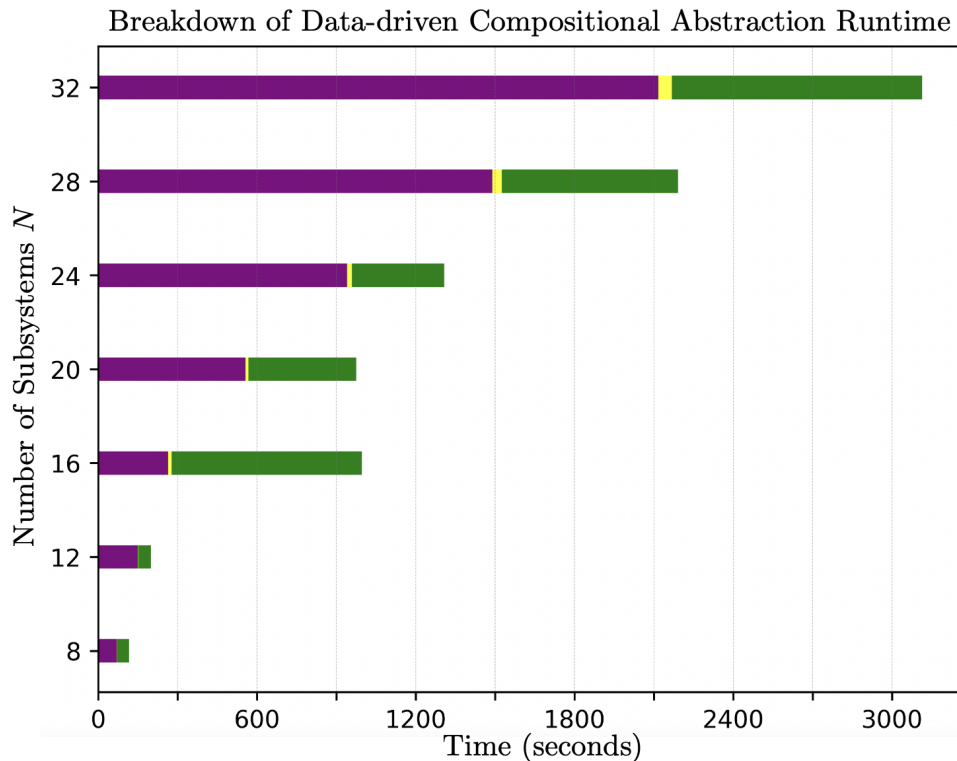


FIGURE 4. The runtime in seconds for systems in (5.1) and interconnection in (5.2) are shown for varying  $N$ . The cumulative runtime is represented by the horizontal bar, segmented into three colors: purple (left) represents abstracting and stacking of the abstraction BDD representations for all subsystems, yellow (middle) denotes the time for approximating the interconnection, and green (right) indicates composing the subsystems and interconnection abstractions.

maintains a state within the consensus region defined by:

$$(5.5) \quad \varphi = \bigvee_{\phi \in [0;31]} \left( \bigwedge_{i=1}^N (\|x_i - \phi\| \leq 2.5) \right).$$

This signifies that all agents have states  $x_i$  within a neighborhood of a common value  $\phi$ . Once the consensus region is attained, the value of  $\phi$  may still change over time as the interconnected system evolves. If  $\phi$  was a known and fixed constant, achieving this objective would be trivially decomposable into  $N$  distinct tasks, and a controller could be synthesized for each subsystem independently. However, because  $\phi$  may vary and is not predetermined, it becomes non-trivial to synthesize a controller for each subsystem  $\Xi_i$  individually, particularly if the controllers only have access to the local state  $x_i$ . The reach and remain objective can be succinctly expressed in a temporal logic formula as  $\diamond\Box\varphi$  [BK08].

Two inherent subsystem's properties exhibit challenges in achieving  $\diamond\Box\varphi$ . Firstly, with fixed values of  $u_i = 0$  and  $w = 0$ , system (5.4) has an unstable equilibrium at  $x_i^* = 16$  and two stable equilibria at  $x_i^* = 1.45$  and  $x_i^* = 30.5$ . This bimodal behavior introduces difficulties, particularly, when the subsystems have initial states both above and below 16, leading to divergence. Secondly, the interaction between the subsystems adds

complexity. The concrete interconnection map is defined as the average state among all subsystems:

$$(5.6) \quad w = \frac{1}{N} \sum_{i=1}^N x_i,$$

where  $w \in [0, 32]$ ,  $\forall [x_1; \dots; x_N] \in \prod_{i=1}^N \mathcal{X}_i$ . If  $u_i(k) = 0$ , then the term  $0.1(x_i - w)$  acts to push the state  $x_i$  away from the average, destabilizing the consensus region  $\varphi$ .

Here, we consider a network of 8 subsystems described by (5.4) and interconnected with (5.6). Hence, the exogenous input  $w$  relies on 8 values (cf. Fig. 3 (top)), making the construction of the interconnection abstraction in a monolithic way very difficult. To address this, we collect 100 and 20 data points (denoted as  $\mathcal{N}_{C_i}$  for the subsystems and  $\bar{\mathcal{N}}_I$  for the interconnection) using the models in (5.4) and (5.6). Furthermore, we estimated the Lipschitz constants as  $\mathcal{L}_{x_i} = \mathcal{L}_{w_i} = 1.599$  and  $\mathcal{L}_{\mathcal{M}} = \frac{1}{8}$  (cf. Remark 4.1). The abstract sets  $\hat{\mathcal{X}}_i$  and  $\hat{\mathcal{U}}$  were generated using grid parameters  $\eta_{x_i} = \eta_w = 0.5$ , while the abstract external input set for subsystems was defined as  $\hat{U}_i = [U_i]_1$ . To construct the interconnection abstraction  $\hat{\mathcal{T}} = (\prod_{i=1}^8 \hat{\mathcal{X}}_i, \hat{\mathcal{U}}, \hat{\mathcal{M}})$ , we solved (4.9) using  $\bar{\mathcal{N}}_I$  sampled input-output data points obtained from (5.6). Upon obtaining  $\bar{\mathcal{M}} \in \mathbb{R}^8$  picking  $\sigma = 4$ , we applied a decomposition of the form  $M_1 := 4\bar{\mathcal{M}} \cdot [\mathbf{1}_8 \ \mathbf{1}_8]$  and  $M_2 := 2\bar{\mathcal{M}} \cdot [\mathbf{1}_8 \ \mathbf{1}_8 \ \mathbf{1}_8 \ \mathbf{1}_8]$  to introduce the following intermediate variables. For any  $[x_1; \dots; x_8] \in \prod_{i=1}^8 \hat{\mathcal{X}}_i$ , we define:

$$(5.7) \quad \begin{aligned} z_1 &= M_2 \cdot [x_1; x_2; x_3; x_4]^\top \in [\mathcal{X}_i]_2, \\ z_2 &= M_2 \cdot [x_5; x_6; x_7; x_8]^\top \in [\mathcal{X}_i]_2, \\ w &= M_1 \cdot [z_1; z_2]^\top \in \hat{\mathcal{U}}. \end{aligned}$$

The abstract interconnected system has  $1.406 \times 10^{12}$  states and the consensus region  $\varphi$  encompasses  $9.49 \times 10^6$  discrete states. The processes of abstracting and stacking of the abstraction BDD representations of the subsystems took 15.28s, and constructing the interconnection abstraction took 3.89s. Then, we synthesized a controller on the interconnected abstraction, with the objective of persistently maintaining the system within the  $\varphi$  region. At each state  $\hat{x} \in \prod_{i=1}^8 \hat{\mathcal{X}}_i$ , the controller provides a set of permissible inputs  $C(\hat{x}) \subseteq \hat{U}$ . Ensuring  $\hat{u}(k) \in C(\hat{x}(k))$  for all time steps guarantees satisfaction of the specification for the interconnected system. As demonstrated, the controller effectively ensures the persistence of the interconnected system's trajectory within region  $\varphi$ , as depicted in Fig. 5. The controller's domain encompasses  $70.6 \times 10^9$  states. Fig. 5 illustrates two sets of trajectories corresponding to an inactive controller and an enforcing controller, which respectively violate and ensure satisfaction of  $\diamond\Box\varphi$ . In Fig. 5, control inputs  $\hat{u}(k)$  are randomly selected from  $C(\hat{x}(k))$ .

## APPENDIX A. DATA-DRIVEN ESTIMATION OF LIPSCHITZ CONSTANT

In this section, we leverage the results presented in [WZ96] to introduce the following algorithm for estimating the Lipschitz constants of the dynamics and the interconnection map. This is accomplished using a finite set of data points collected from the system.

Through the implementation of Algorithm 5, the Lemma A.1, sourced from [WZ96], guarantees that the estimated Lipschitz constant converges towards its actual value in the limit.

**Lemma A.1.** *Consider a dt-CS  $\Xi$  with unknown transition function. By applying Algorithm 5, the estimated Lipschitz constants,  $\mathcal{L}_x$  and  $\mathcal{L}_w$ , converges to their actual value if and only if  $\delta$  gets arbitrarily small and  $P, L$  becomes very large.*

*Remark A.2.* It is important to note that we do not consider any confidence bound for estimating the Lipschitz constants in our approach. Instead, we choose a very small value for  $\delta$  and use large values for  $P$  and  $L$ . This way, Algorithm 5 can give us a very accurate estimate for the Lipschitz constant. In addition, it is worth mentioning that one can modify Algorithm 5 to estimate the Lipschitz constant  $\mathcal{L}_{\mathcal{M}}$  for the interconnection map.



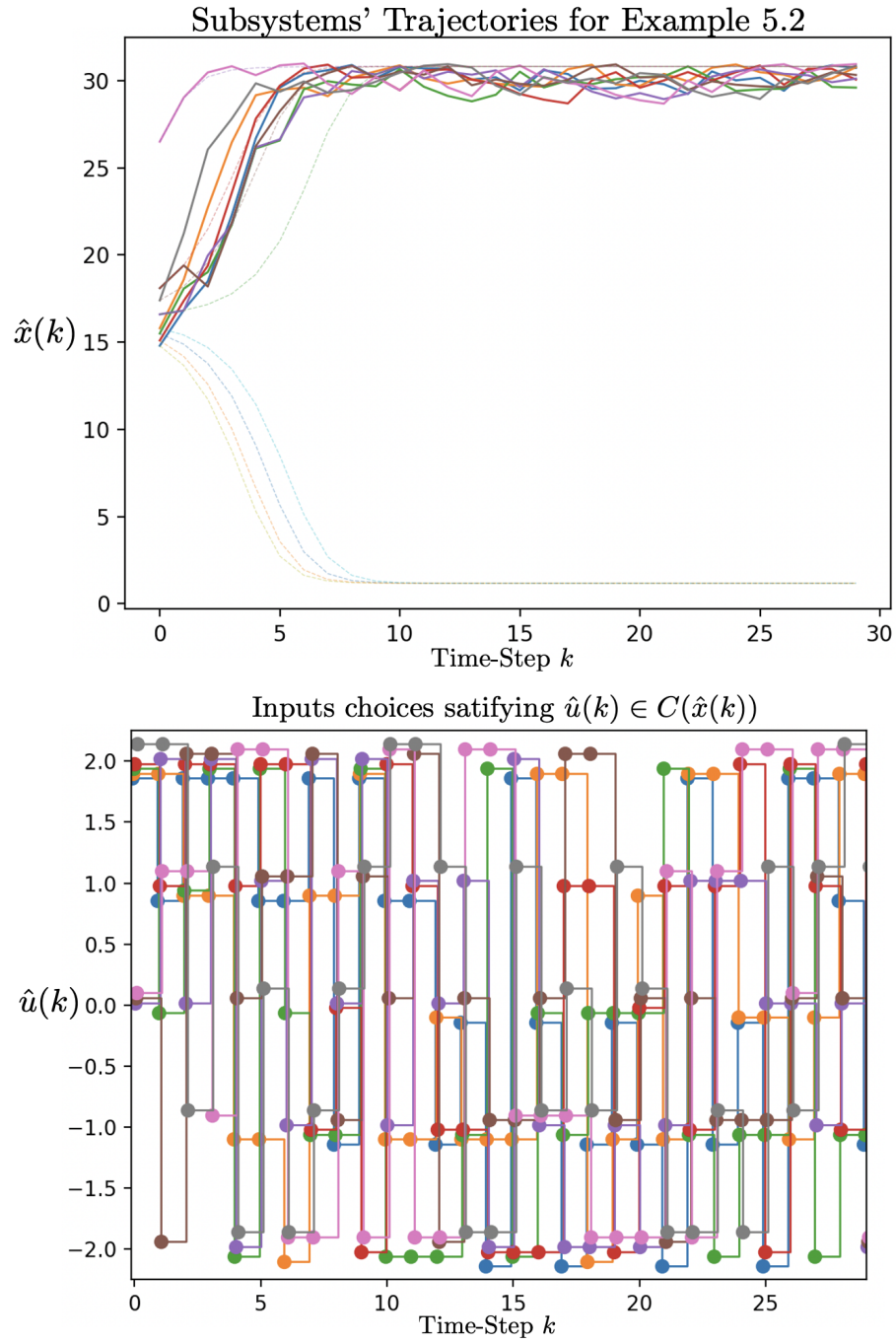


FIGURE 5. The top sub-figure depicts two 8-dimensional trajectories, which are illustrated as two sets of eight scalar-valued trajectories. Each line represents a trajectory  $x_i(k)$  for  $i \in [1; 8]$ . Solid lines correspond to a controller enforcing  $\Diamond\Box\varphi$ , while dashed lines represent an inactive controller with  $u_i(k) = 0$  for all systems  $i$  and time steps  $k$ . Both sets of trajectories initiate from the same initial state  $x[0] = [14.8; 15.8; 15.5; 15.1; 16.6; 18.1; 26.5; 17.4]$ , which lies outside the consensus region  $\varphi$  and supports the bimodal property of (5.4). The bottom sub-figure depicts the piecewise constant control inputs required to enforce  $\Diamond\Box\varphi$ . The depiction is with slight vertical and horizontal perturbations for visual clarity.

**Algorithm 5** Estimation of Lipschitz constant for dt-CS

- 
- 1: For a given input  $\hat{u} \in U$ , select  $P, L \in \mathbb{N}$  with points  $x_l, \bar{x}_l \in \hat{X}$  such that  $\|x_l - \bar{x}_l\| \leq \delta \forall l \in [1; L]$  where  $\delta > 0$
  - 2: **for**  $j \in [1; P]$  **do**
  - 3:   **for**  $l \in [1; L]$  **do**
  - 4:     Simulate the dt-CS from initial states  $x_l$  and  $\bar{x}_l$  in one time-step to obtain  $x'_l$  and  $\bar{x}'_l$ , respectively
  - 5:     Compute slope  $\Delta_l := \|x'_l - \bar{x}'_l\| / \|x_l - \bar{x}_l\|$
  - 6:   **end for**
  - 7:   Obtain the maximum slope  $\Delta_j^* := \max\{\Delta_1, \dots, \Delta_L\}$
  - 8:   Fit  $\{\Delta_1^*, \dots, \Delta_P^*\}$  into a Reverse Weibull distribution [WZ96] to obtain the parameters termed location, scale and shape
  - 9: **end for**
  - 10: The estimated Lipschitz constant  $\mathcal{L}_x(\hat{u})$  is the obtained *location* parameter
- 

## APPENDIX B. PROOF OF LEMMA 4.5

*Proof.* We establish the proof by contradiction. Suppose (4.4) does not hold, *i.e.*,  $\|\vartheta_1(\hat{x}, \hat{u}, \hat{w})\| > \mathcal{L}_x(\hat{u})$ . Then by applying (4.3), it holds that  $\forall x' \in \mathcal{X}, \forall \hat{x} \in \hat{X}$  and given  $(\hat{u}, \hat{w}) \in \hat{U} \times \hat{W}$  with  $w_1, w_2 \in \Phi_{\eta_w/2}(\hat{w})$ ,

$$\begin{aligned} \|\vartheta_1(\hat{x}, \hat{u}, \hat{w})\| > \mathcal{L}_x(\hat{u}) &\geq \frac{\|f(x', \hat{u}, w_1) - f(\hat{x}, \hat{u}, w_2)\|}{\|x' - \hat{x}\|} \\ &\quad - \frac{1}{2} \mathcal{L}_w(\hat{u}) \frac{\|\eta_w\|}{\|x' - \hat{x}\|}. \end{aligned}$$

The latter inequality leads to

$$(B.1) \quad \|f(x', \hat{u}, w_1) - f(\hat{x}, \hat{u}, w_2)\| \leq \|\vartheta_1\| \|x' - \hat{x}\| + \mathcal{L}_w(\hat{u}) \|\eta_w\|.$$

By employing (4.1), (4.2), and then applying the infinity norm on the resulting inequality, one obtains

$$(B.2) \quad \|f(x', \hat{u}, w_1) - f(\hat{x}, \hat{u}, w_2)\| \leq \|\vartheta_1\| \|x' - \hat{x}\| + \|\vartheta_2\|.$$

By subtracting (B.1) from (B.2), and without loss of generality suppose that  $\mathcal{L}_w(\hat{u}) \|\eta_w\| > 1$ , one has  $1 \leq \|\vartheta_2\|$ , which does not hold for every  $\vartheta_2 \in \mathbb{R}_{\geq 0}^{\dim(\mathcal{X})}$  and, thus, concludes the proof.  $\square$

## REFERENCES

- [ALZ23] Daniel Ajeleye, Abolfazl Lavaei, and Majid Zamani. Data-driven controller synthesis via finite abstractions with formal guarantees. *IEEE Control Systems Letters*, 7:3453–3458, 2023.
- [AMP22] Daniel Ajedamola Ajeleye, Tommaso Masciulli, and Giordano Pola. Output feedback control of nondeterministic finite-state systems with reach-avoid specifications. In *2022 30th Mediterranean Conference on Control and Automation (MED)*, pages 1012–1017. IEEE, 2022.
- [AZ24] Daniel Ajeleye and Majid Zamani. Data-driven controller synthesis via co-büchi barrier certificates with formal guarantees. *IEEE Control Systems Letters*, 2024.
- [BK08] Christel Baier and Joost-Pieter Katoen. *Principles of model checking*. MIT press, 2008.
- [Bry86] Randal E Bryant. Graph-based algorithms for boolean function manipulation. *Computers, IEEE Transactions on*, 100(8):677–691, 1986.
- [CPMJ22] Rudi Coppola, Andrea Peruffo, and Manuel Mazo Jr. Data-driven abstractions for verification of deterministic systems. *arXiv preprint arXiv:2211.01793*, 2022.
- [FQMV17] Chuchu Fan, Bolun Qi, Sayan Mitra, and Mahesh Viswanathan. DryVR: Data-driven verification and compositional reasoning for automotive systems. In *International Conference on Computer Aided Verification*, pages 441–461. Springer, 2017.
- [FS18] Salar Fattahi and Somayeh Sojoudi. Data-driven sparse system identification. In *2018 56th Annual Allerton Conference on Communication, Control, and Computing (Allerton)*, pages 462–469. IEEE, 2018.
- [GKA17] Felix Gruber, Eric S Kim, and Murat Arcak. Sparsity-aware finite abstraction. In *2017 IEEE 56th Annual Conference on Decision and Control (CDC)*, pages 2366–2371. IEEE, 2017.

- [HAT17] Omar Hussien, Aaron Ames, and Paulo Tabuada. Abstracting partially feedback linearizable systems compositionally. *IEEE Control Systems Letters*, 1(2):227–232, 2017.
- [HW13] Zhong-Sheng Hou and Zhuo Wang. From model-based control to data-driven control: Survey, classification and perspective. *Information Sciences*, 235:3–35, 2013.
- [KAZ18] Eric S Kim, Murat Arcak, and Majid Zamani. Constructing control system abstractions from modular components. In *Proceedings of the 21st International Conference on Hybrid Systems: Computation and Control (part of CPS Week)*, pages 137–146, 2018.
- [KMS<sup>+</sup>22] Milad Kazemi, Rupak Majumdar, Mahmoud Salamati, Sadegh Soudjani, and Ben Wooding. Data-driven abstraction-based control synthesis. *arXiv preprint arXiv:2206.08069*, 2022.
- [LF22] Abolfazl Lavaei and Emilio Frazzoli. Data-driven synthesis of symbolic abstractions with guaranteed confidence. *IEEE Control Systems Letters*, 7:253–258, 2022.
- [Lju98] Lennart Ljung. System identification. In *Signal analysis and prediction*, pages 163–173. Springer, 1998.
- [MGF21] Anas Makdesi, Antoine Girard, and Laurent Fribourg. Efficient data-driven abstraction of monotone systems with disturbances. *IFAC-PapersOnLine*, 54(5):49–54, 2021.
- [MGW17] Pierre-Jean Meyer, Antoine Girard, and Emmanuel Witrant. Compositional abstraction and safety synthesis using overlapping symbolic models. *IEEE Transactions on Automatic Control*, 63(6):1835–1841, 2017.
- [RWR16] Gunther Reissig, Alexander Weber, and Matthias Rungger. Feedback refinement relations for the synthesis of symbolic controllers. *IEEE Transactions on Automatic Control*, 62(4):1781–1796, 2016.
- [RZ16] Matthias Rungger and Majid Zamani. SCOTS: A tool for the synthesis of symbolic controllers. In *Proceedings of the 19th international conference on hybrid systems: Computation and control*, pages 99–104, 2016.
- [SLSZ24] Ali Salamati, Abolfazl Lavaei, Sadegh Soudjani, and Majid Zamani. Data-driven verification and synthesis of stochastic systems via barrier certificates. *Automatica*, 159:111323, 2024.
- [Som97] Fabio Somenzi. CUDD: CU decision diagram package. *Public Software, University of Colorado*, 1997.
- [Tab09] Paulo Tabuada. *Verification and control of hybrid systems: a symbolic approach*. Springer Science & Business Media, 2009.
- [WZ96] GR Wood and BP Zhang. Estimation of the lipschitz constant of a function. *Journal of Global Optimization*, 8:91–103, 1996.
- [XZEL20] Bai Xue, Miaomiao Zhang, Arvind Easwaran, and Qin Li. PAC model checking of black-box continuous-time dynamical systems. *IEEE Transactions on Computer-Aided Design of Integrated Circuits and Systems*, 39(11):3944–3955, 2020.

DEPARTMENT OF COMPUTER SCIENCE, UNIVERSITY OF COLORADO BOULDER, USA

*Email address:* {daniel.ajeleye, majid.zamani}@colorado.edu

*URL:* <https://www.hyconsys.com/members/dajeleye/>

*URL:* <https://www.hyconsys.com/members/mzamani/>